Preparation and studying of radiation effect on $Bi_{2-x}Pb_xSr_2Ca_{n-1}Cu_{n-y}Ni_yO_{2n+4+\sigma}$ high temperature superconductor

A thesis submitted to

The Council of the College of Education for Pure Science (Ibn Al-Haitham)

University of Baghdad as a Partial Fulfillment of Requirements

for Degree of Master in the Physics Science

Submitted by the student

Mohammed Abdulmohsin Ali

Supervised by

Prof.Dr. Kareem Ali Jasim

2018 A.D.   *1439 A.H.*

بسم الله الرحمن الرحيم

((وَقَالُوا الْحَمْدُ لِلَّهِ الَّذِي صَدَقَنَا وَعْدَهُ
وَأَوْرَثَنَا الْأَرْضَ نَتَبَوَّأُ مِنَ الْجَنَّةِ حَيْثُ نَشَاء
فَنِعْمَ أَجْرُ الْعَامِلِينَ))

صدق الله العظيم

Supervisors Certification

I certify that this thesis entitled (**Preparation and studying of radiation effect on** $Bi_{2-x}Pb_xSr_2Ca_{n-1}Cu_{n-y}Ni_yO_{2n+4+\delta}$ **high temperature superconductor**) was prepared by **Mohammed Abdulmohsin Ali** under my supervision at the Physics Department, College of Education for pure Science Ibn-Al-Haitham, University of Baghdad as partial fulfillment requirements for the degree of Master of Science in physics.

Signature:

Name: **Dr. *Kareem Ali Jasim***

Title: professor

Address: College of Education for pure Science Ibn-Al-Haitham, University of Baghdad

Date: / /2018

Certification of the Chairman of physics department

In view of the available recommendations, I forward this thesis for debate by the Examination Committee.

Signature: S.A.MAKI

Name:*Dr. Samir Ata Maki*

Title: Professor

Address: Chairman of Physics Department, College of Education for pure Science Ibn-Al-Haitham, University of Baghdad

Date: / /2018

Committee Certification

We certify that we have read this thesis "**Preparation and studying of radiation effect on** $Bi_{2-x}Pb_xSr_2Ca_{n-1}Cu_{n-y}Ni_yO_{2n+4+\delta}$ **high temperature superconductor**" submitted by (**Mohammed Abdulmohsin Ali**) and as examining committee examined the student in its content and that in our opinion it is adequate with standard as thesis for the Degree of Master of Science in Physics.

Signature:

Name: *Asst.Prof. Dr.Akram R. Jabur*

Address: Department of materials Eng. University of Technology

(Chairman)

Date: /   / 2018

Signature:

Name: *Asst. Prof. Dr. Abbas K. Saadon*

Address: Collage of education for pure science Ibn al-Haitham, University of Baghdad
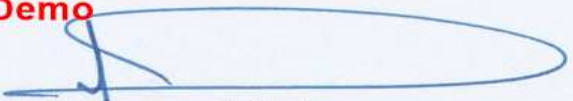
(Member)

Date: /   / 2018

Signature:

Name: *Dr. Shatha H. Mahdi*

Address: Collage of education for pure science Ibn al-Haitham, University of Baghdad

(Member)

Date: /   / 2018

Signature:

Name: *Prof. Dr. kareem A. Jasim*

Address: Collage of education for pure science Ibn al-Haitham, University of Baghdad

(Member-Supervisor)

Date: /   / 2018

Approved by the Council of the College of Education for Pure Sciences Ibn-Al-Haitham / University of Baghdad

Signature:

Name: *Asst. Prof. Dr. Hasan Ahmed Hasan*

Address: **Dean of college**

Date: /   / 2018

List of tables

List of symbols

symbol	Description	Unit
HTS	High Temperature superconductor.	/
T_c	Critical temperature .	K
H_c	Critical magnetic field	T
J_c	Critical current density	A/m^2
μ_0	Permeability of free space	H/m
B_c	Magnetic flux density	T
λ	Penetration depth	Cm
v_F	Fermi level velocity	m/s
H	External magnetic field	T
m	Mass of electron	Kg
n_s	The Local density of superconducting carriers	$Carrier/Cm^3$
ξ	The coherence length	Cm
K	Ginzburg-landau factor	/
J_s	Super current density	A/m^2
υ_s	Velocity of super pairs	m/S
m_s	Mass of super electron	Kg
μ_s	Permeability of super charge	H/m
E	Electric field intensity	V/m
Δ	Superconductor energy gap	eV
$\Delta_{(0)}$	Superconductor energu gap at OH	eV
BSCCO	BiSrCaCuO	/
a,b,c	Lattice parameters constant	A°
δ	oxygen content magnitude	/
λ	Wave length	A°
h,k,L	Miller indices	/
θ_{hkl}	Diffraction angles	Degree
r	Radius of pellet	Cm
L	Length of sample vetween two probe	Cm
ρ	Electrical resistivity	$\Omega.m$
W	pellet width	Cm
τ	Crystallite size	nm
d	Full width half maximum (F.W.H.M.)	Degree
M_A	Molar mass of the sample	g/mol
M_B	Molecular weight of sodium thiosulfate solution	g/mol
m_A	Weight of sample	g

Chapter One

Introduction to superconductivity

Chapter One

Introduction to Superconductivity

1.1 Introduction:

Superconductivity is one of phenomena that represent two states, that inherently correlated, namely, ideal conductivity(R=0) and diamagnetic ($\mu < 1$) [1], where this phenomenon occurs with certain substances. It was observed that these materials lose theirs electrical resistivity suddenly to reach a zero value at certain low temperatures called critical temperature and has a symbol of (T_c) Represents the threshold for superconductivity, but is not the only criterion for the realization of superconductivity, there are two other criteria, namely, critical magnetic field(H_c) and critical current density(J_c) [2].

1.2 Historical review:

In 1908, the Dutch scientist Kamerlingh Onnes succeeded in liquefying helium gas by put it under pressure. The temperature in which the helium gas was converted into liquid is (4.2K) or (- 296 C^{o}) [1] [3] [4]. Kamerlinghs success was followed, where In1911, he found that the electrical resistance of mercury decreases to the zero abruptly when the temperature is reduced to a value of (4K), this observation came when he studied the electrical properties of mercury and the electrical resistance of some materials [5, 1]. In 1912 Kamerlinghs explored that when the superconductors exposed to high magnetic field they get back theirs resistivity. In 1913 a new superconductor element was explored, where lead (Pb) was explored to serve as superconductor at (7.2K) [5]. The most important property beside the zero resistivity is the diamagnetic behavior owned by superconductor where it is explored by Meissner and

Ochsenfeld in 1933 through them observation of magnetic field exclusion by superconductor under it's T_c [[5, 6, 7]. Scientists have tried to detect superconducting materials with higher critical temperatures, but this was futile as they did not exceed 10K until the early 1940s. Where the Niobium compound (NbN), was discovered which has a critical temperature of 15K. The most important theory in the field of superconductivity is the BSC theory, which was complied with by the two scientists J.Barden, Cooper and Schrieffer in 1957, as it is a theory that deals with the subject of attraction between the electrons of superconducting material when cooled under the critical temperature of its superconducting state transition [5, 8, 9]. The situation has remained the same until 1973s where the (Nb_3Ge) compound, was detected which has a critical temperature of 23K [10, 11]. The most important event was the discovery of the ceramic superconductor in 1986s, where the preparing of the (La-Ba-Cu-O) compound was achieved by the two scientists (J.George Bednorz and Karl Alex Muller) with a critical transition temperature of 30k. Chu's group succeeded in reaching a critical temperature of 92k in 1987 by replacement of the element of lantium (La) with the element of etherium(Y) and the obtaining of a superconductor from the (Y-Ba-Cu-O) system, which exceeded the liquid nitrogen boiling temperature of 77K, this discovery was a remarkable development in the history of superconductors [10, 12]. In 1988, Bi-Sr-Ca-Cu-O (BSCCO) superconducting system was discovered by Maeda et al , with a critical transition temperature of more than 100 K, this compound was prepared with chemical form of $Bi_2Sr_2Ca_2Cu_3O_{2n+4+\delta}$ and indicated by Bi(22 (n-1) n) , where n=1,2 and 3 have $T_{c=}$ 22K , 80K and 110K respectively [5, 12] .And then reached a critical temperature equal to 133K by preparing $Hg\,Ba_2Ca_2Cu_3O_{2n+4+\delta}$ system in 1993s [13]. The critical temperature of $Hg\,Ba_2Ca_2Cu_3O_{2n+4+\delta}$ system

increased to reach 164k by applying high pressure in the same year [14, 5].

1.3 <u>Superconductor properties:</u>

In order to achieve superconductivity, three basic conditions must be met simultaneously, these conditions are: reach the critical temperature magnitude (T_c), critical current density magnitude (J_c) and critical magnetic field (H_c). Figure (1-1) demonstrates the relation among these three conditions.
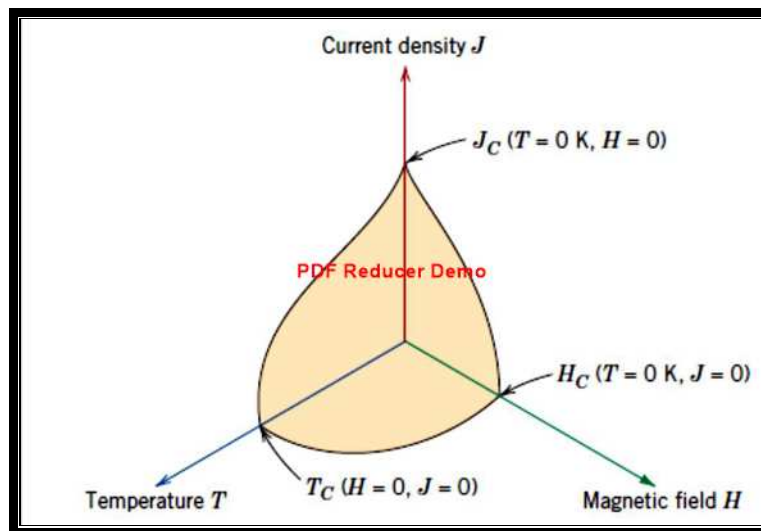
Figure1- 1: The relation among Tc, Hc and Jc [5]

1.3.1 <u>Critical temperature (T_c):</u>

The supercondoctors substances translate to supercondecting state when their temperature decreas to characterestic temperature called critical temperature(T_c), the critical temperature is the temperature at which the electrical resistivity decreases suddenly to zero [15]. The superconducting state described by BSC theory, some of these substanses translate to superconducting state at low temperature until exploration of high temperature superconductor materials in 1986, these materials have critical temperature in range of 120K. Because to its

ability to serve as superconductotr substance in a temperature higher than the boiling point of liquid nitrogen (77K) [16].
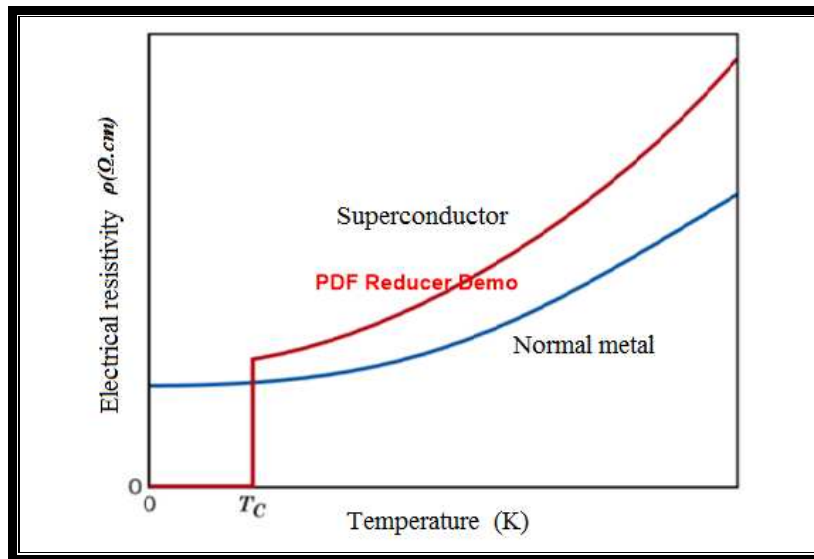
Figure1- 2: Relation between absolute temperature and electrical resistivity of normal and superconducting state [5].

1.3.2 Critical current density(J_c):

If the magnitude of electric current pass through the superconductor substance rais to certain magnitude higher than certain magnitude ,the superconductor will retain to the normal state even if its temperature less than its critical temperature [16], hence the critical current can defined as the highest magnitude of current can pass through the superconductor substance without retain to its normal state [17, 5]. There is invers proportional between critical current density and critical temperature as illustrated in Figure(1-1) [16].

1.3.3 Critical magnetic field (H_c):

When the superconductor substancs cooled below its critical temperature and the magnatic field increase around the substance, the magnetic field was repelled and remain arround the substance until reach the particular magnitude at which the magnetic field pentrates the

substance [15]. The highest magnitude of magnetic field over which the resistance increace and the substance back to normal state even if its temperature less than its critical temperature is called critical magnetic fieldH_c [17]. The relation between the critical magnetic field and critical temperature is inversly relation as demonstrated in Figure(1-3) and given by following equation [2] :

$$H_c = H_c(0) \left[1 - \left(\frac{T}{T_c}\right)^2\right] \ldots\ldots\ldots\ldots\ldots (1\text{-}1)$$

Where:

H_c: Maximum critical field (Tesla), $H_c(0)$: Maximum critical field (Tesla)
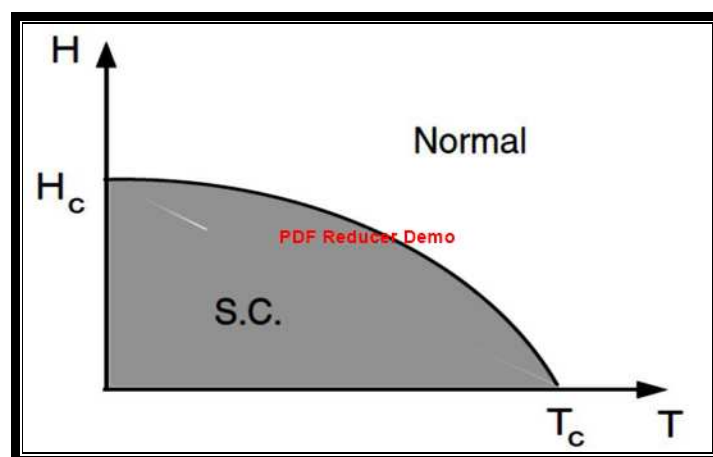
Figure1- 3 Relation between critical temperature and critical magnetic field [18].

1.4 Meissner effect:

In 1933 , the two germane scientists W. Meissner and R. Ochsenfeld noticed that when the superconductor substances exposed to external magnetic field(B_{ext}) and cooled under its critical temperature ,the magnetic flux line cannot penetrate the substance thickness and a repel arises between the substance and the external magnetic field i.e. the

magnetic field inside the substance equal zero (B_{in}), this means that the superconductor substance behave as a perfect diamagnetic substance has magnetic permeability equal to zero. But there is a particular magnitude of magnetic field over which the magnetic field penetrates the substance until if it below T_C this particular magnetic field magnitude called critical magnetic field B_c [19]. Meissner effect happens because that the external field induces screening current on a surface, this current creates interior field which directed to perfectly revocation the applied field [20] [21] [22]. Figure (1-4) illustrates meissner effect.

$B_{in}=B_{ext}+B_{induced}$ ……………..…………(1-2)

$B_{in} =\mu_\circ H+\mu_\circ M$ …………………..…….(1-3)

$B_{in} =\mu_\circ H(1+\chi_m)$ ………………..………(1-4)

Where

B_{in} : The magnetic field inside the superconductor, B_{ext} : The external magnetic field, $B_{induced}$: The interior magnetic field of the superconductor. All of B_{in}, B_{ext} and $B_{induced}$ have units of Tesla

But B = 0 in the superconductors, this mean :

M = - H, $\chi_m = - 1$

$B_{in}= 0$

Where:

$\mu_\circ$: Permeability of free space which has units of H/m, M: Magnetization which has units of A/m, χ_m : The magnetic susceptibility, H : External magnetic field .
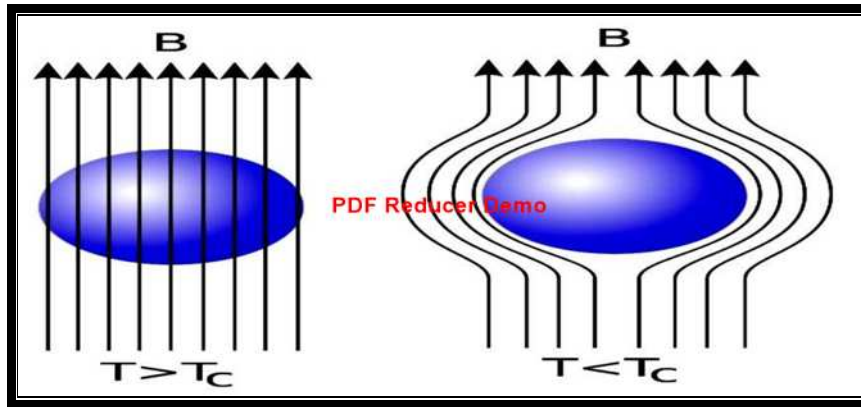
Figure1- 4: Explaination of meissner effect [5].

1.5 Basics concept in superconductivity:

1.5.1 Coppers pairs:

Cooper pairs are the charges carriers in superconductor substances, it was created when the electron with momentum coupled with the another one of precisely contrary momentum and spin .This coupling take place when the superconductor substances cooled to temperature less than its critical temperature, the normal state of free electron gas was converted to a quantum fluid of coherent electrons pairs in reciprocal space [23] [24].

1.5.2 Coherence length (ξ) :

Coherence length is the distance over which the coopers pair stay together, thus the superconductivity state depend strongly on the coherence length. In 1953 Pippad suggested the coherence idea, [25, 15]and discovered that the superconductor substance density changes as coherence length change. Almost superconductor metals have coherence length about$(10^{-4}cm)$. The coherence length is scale of distance between two superconductivity electrons as given in the following equation [5]:

$\xi = \frac{h v_F}{2\Delta}$ …………………….……(1-5)

Where, $v_{F:}$ The electron velocity at Fermi level which has units of m/s, 2Δ: The energy gap which has units of eV.

1.5.3 Penetration depth(λ):

The magnetic field can penetrate small region near the superconductors surface, this limited depth region called penetration depth (λ), the magnitude of penetration depth ranging usually between 10^{-8} and 10^{-7}m, which changes with temperature changing as given in the following equation [19] :

$$\lambda_L = \lambda_\circ \left[1 - \left(\frac{T}{T_c} \right)^4 \right]^{\frac{-1}{2}} \ldots\ldots\ldots\ldots\ldots..(1\text{-}6)$$

Where: $\lambda_\circ$ is the penetration depth at absolute zero temperature which has units of Cm.

This equation shows that the penetration depth magnitude go to infinity ($\lambda \rightarrow \infty$) when the temperature equal to superconductor critical temperature (T=T_C). That means when the temperature increase until reach the critical temperature and the substance transform to normal state and the field completely penetrate the substance [26].

The equation (1-7) can used to determine the superconductor type [2]:

$$K = \frac{\lambda}{\xi} \ldots\ldots\ldots\ldots\ldots\ldots\ldots\ldots\ldots\ldots\ldots.(1\text{-}7)$$

Where: K is the Ginzburg-landau factor. Now, if ($k < \frac{1}{\sqrt{2}}$) , then the superconductor (type I), but if ($k > \frac{1}{\sqrt{2}}$) , then the superconductor (type II) [27, 28]. And the magnetic field inside the superconductor relate with penetrate depth by the following equation [2]:

$$B_{(X)} = B_\circ e^{\frac{-X}{\lambda}} \ldots\ldots. \ldots\ldots\ldots\ldots\ldots(1\text{-}8)$$

Where: $B_\circ$ is the magnetic field at the surface, X: is the distance from the surface to particular point inside the substance.

Figure (1-5) explains the behavior penetration depth and coherence length in both normal and superconducting state.
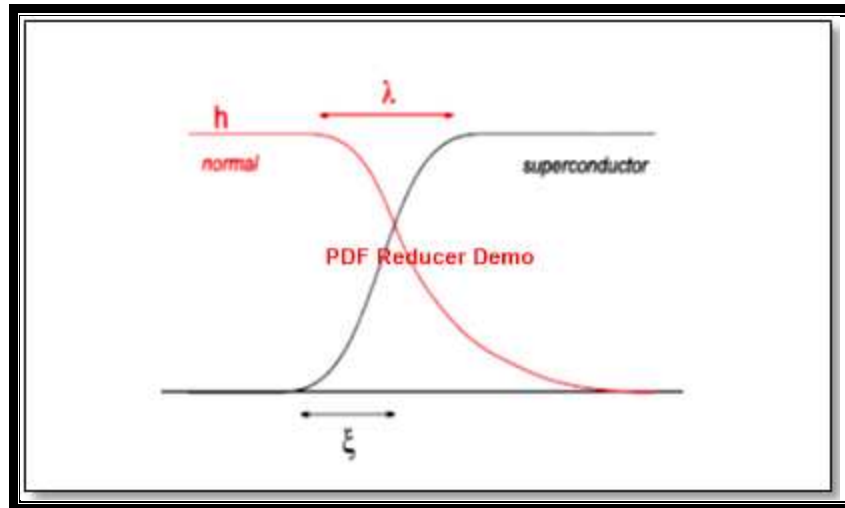
Figure1- 5: Pentration depth and coherence length of normal and superconducting state [5].

1.6 Theories of superconductor at low temperature:

1.6.1 London equation:

The conduction electrons in metal in normal state were described by ohm's low which was expressed by mathematical formula: (j=σE) but after modification this description due to Meissner effect in the superconductivity state, it was assumed that in the superconductivity state the current density proportional directly with potential vector(A) of magnetic field [15].

B=∇XA…………………………... (1-9)

And the proportional constant is $(\frac{-1}{\mu_0 \lambda_L^2})$ [29, 15].

$J = (\dfrac{-1}{\mu_0 \lambda_L{}^2}) A$ …………………….(1-10)

Where: λ_L is the dimensions length constant.

By taking curl for both sides:

$\nabla \times J = (\dfrac{-1}{\mu_0 \lambda_L{}^2}) B$ …………………..(1-11)

By utilize Maxwell equation:

$\nabla \times B = \mu_\circ j$ …………………..….. (1-12)

$\nabla \times \nabla \times B = \mu_\circ \nabla \times j$ … …. … … (1 − 13)

Thus:

$\nabla \times \nabla \times B$ = *grad div B* - $\nabla^2 B$ …… *(1-14)*

$\nabla \times \nabla \times B$ = -$\nabla^2 B$ (because (div B) =0)*………(1-15)*

$-\nabla^2 B = \mu_\circ \nabla \times j$ *……………….… (1-16)*

$-\nabla^2 B = -\left[\dfrac{n_s\, e^2\, \mu_\circ}{m^*}\right] B = -\dfrac{B}{\lambda^2}$ *……… (1-17)*

$\lambda_L{}^2 = -\left(\dfrac{n_s\, e^2\, \mu_\circ}{m^*}\right)$ *……… (1-18)*

Where: λ is the London penetration depth (this parameter depend on the depth that the magnetic field penetrate it) .

      By joining this concept with gorter and casmer formula which describe the relation between penetration depth and temperature   [30]

$\lambda_L = \dfrac{\lambda_{(0)}}{\sqrt{1+t^4}}$…….(1-19)

Equation (1-19) has not microscopic explanation at low temperature, but it was expressed as:

$$\lambda_{T=}\lambda_{(0)}[(1 + \frac{t^4}{2}) + 0(t^8)]........(1\text{-}20)$$

Where $0(t^8)$ is correction factor.

1.7 Ginzburg-Landau theory

Both of Ginzburg and Landau utilized the macroscopic outlook to explain the transition from normal state to superconductor state on the thermodynamic origin in phase transition of second order, and they developed a new parameter, this new parameter called order parameter ψ of electrons of superconductivity n_s, thus the super electrons local density was presented by $n_{s=|\psi|^2}$. Depending on G-L theory, the alteration of free energy (F) can be expressed as an order parameter ψ power series. The magnetic depth of penetration (λ) and coherence length (ξ) expressed as [5]:

$$\xi^2(\text{T}) = \frac{h^2}{4m\alpha} \dots\dots\dots\dots\dots\dots(1\text{-}21)$$

And

$$\lambda^2(\text{T}) = \frac{mc^2}{4\pi n_s e^2} \dots\dots\dots\dots\dots(1\text{-}22)$$

Where: α: is a variable factor depends on the thermodynamic transition of superconducting phase. And the two factors (ξ and λ) diverge by the same manner, T=T_C when T→ T_C the ξ over λ resultant represents particular parameter K called Ginzburg-Landau parameter and is the special parameter of the superconductor material [15].

1.7.1 The Josephson Effect:

When thin oxide insulator substance has a thickness of about (2nm) inserted between two superconductor substance, a current can flow between two separated superconductors passing through insulator

substance. This current flowing attributed to the passing of cooper pairs through the insulator substance by tunneling. This tunneling phenomena explorer experimentally by I.Giaever, while B.D.Josephson demonstrated this phenomena theoretically for a first time [31] [32]. Figure(1-6) illustrates Josephsone junction.
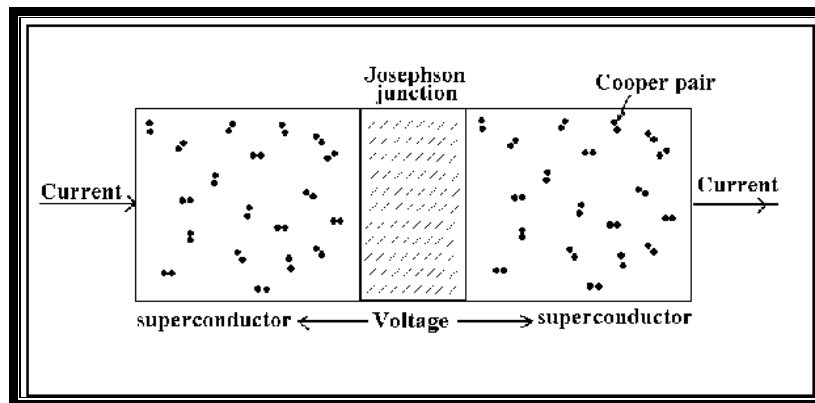
Figure1- 6: Josephsone junction.

1.8 The Microscopic Description Of Superconductivity by BCS Theory:

The understanding of superconductivity phenomena becomes clearer by depending on BCS theory. It is considered as the first theory discussed the superconductivity from the microscopic overview it was suggested via John Barden, Leon Copper and J. Robert Schrieffer in 1957 [33]. BCS theory explained the superconductivity in low temperature, it considered that the electrons which have the opposite moments and spins can coupled and create what called cooper pairs. These electrons pairs can behave unlike the individual electrons which fermions obey to Pauli exclusion principle, the electron pairs generally act as bosons, which may be agglomerate at the same energy level. Due to its low energy level the electrons pair create energy gap less than both of them approximately (1meV) which prevent the collision interaction that caused the normal electric resistivity.

12

1.9 Type-I and type- I I superconductors:

The superconductor substances have been classified into two categories depended on their response to magnetic fields, this classification involves type– I (soft superconductor) and type - I I (hard superconductors) superconductors. The magnitude of Ginzburg-Landau parameter (k) plays important role in compare between two types .where if k$<\frac{1}{\sqrt{2}}$, then the superconductor is type- I, but if k$>\frac{1}{\sqrt{2}}$, then the superconductor is type- II [5] [34].

1.9.1 Type I (or soft) superconductors:

In this type the superconductor substance behave as a perfect diamagnetic substance when its magnetic field magnitude below its critical magnitude (H_C). The substance stays perfect diamagnetic substance until reach the critical magnetic field magnitudeH_C. The substance transform to normal state and full magnetic penetration happen [35] [36]. i.e. showed complete meissner effect. This type usually has low critical magnetic field magnitude about 0.1T as a highest known magnitude, thus this type unsuitable to utilize in high field superconducting magnet [22] [37]. A lot of metal element classified as type I superconductor such as lead, aluminum and mercury.
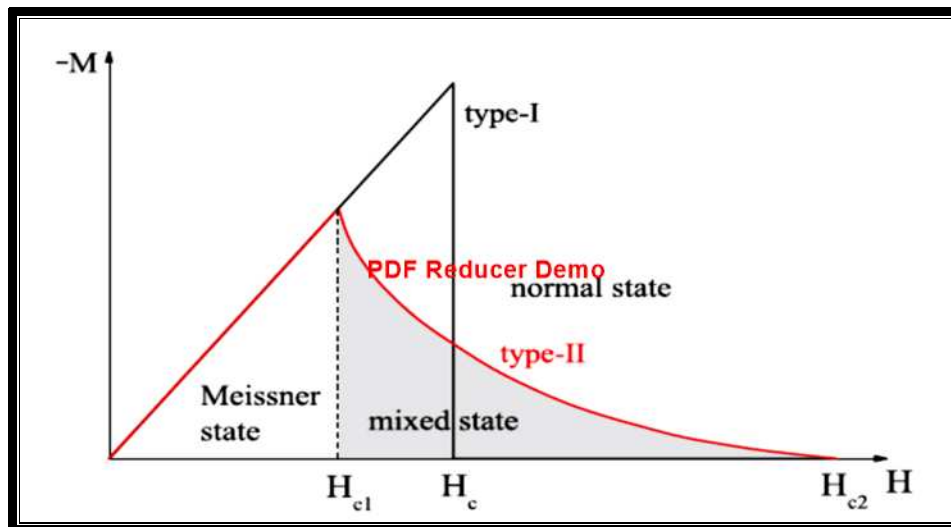
Figure1- 7: Two supercondoctor types behavior [17].

1.9.2 Type II (or hard) superconductors:

In this type the superconductor substances do not display complete meissner effect [38, 5], this substance stays diamagnetic substance until reach the particular magnetic field magnitude H_{c1} at which the magnetic flux line start to penetrate into the bulk of substance , and the penetration running with rising magnetic field magnitude until reach H_{c2} at which the field penetration complete. For field magnitude lies between H_{c1} and H_{c2} the substance exists in a state that called mixed state, it contains normal state and superconducting state [7] [35]. The magnitude of H_{c2} higher than magnitude of H_{c1}, and the critical field of type II substance approximately 100 time than critical field of type I. The magnitude of H_{c2} higher than 30T has been noticed. The behavior of both types of superconductors was illustrated in figure (1-7).

1.10 Influence of isotopes:

The superconductivity is one of phenomena that are sensitive to any changes in electrons system and the electrons system affected by crystal lattice. So the superconductivity properties was influenced by isotope mass changing, because the isotope mass one of important factor

14

which can influence in lattice crystal properties, like the lattice vibration frequencies affected by ion mass. The exploration of isotope effect was first observed by Maxwell where he observed an inverse relationship between the mass of the isotope and the critical temperature of the transition. When substituting one of the atoms of superconducting material with one of the larger ones in the mass, it was noted that the critical temperature of the transition decreased. The critical temperature of the transition varies from 4.185 K to 4.140 K when the mass number changes from 199.5 to 203.4 a.m.u. For mercury, This leads us to conclude a relationship between the peer mass and the critical transition temperature [2]

$M^{\alpha}T_c$= constant …………………(1-23)

Where α:Is exponent of isotope effect.

1.11 Energy gap:

The emergence of a gap in the energy spectrum attributed to the existence of attraction between the internal electrons in superconductors. There will be absorption of energy and electron excitation through the gap when the frequency is sufficiently large and then the pairing process will be useless. This demonstration is fully consistent with the BCS theory. There are some factors can determine the width of the energy gap such as tunneling, electromagnetic absorption and specific heat. The ideal width is approximately less than 1mev. The emergence of this gap does not occur abruptly as it is equal to zero at the critical transition temperature, then increases until reach to 3.5 KT_c at absolute zero temperature. This proportion between energy gap width and temperature was imposed by BCS theory. Figure (1-8) illustrate the relation between gap width and temperature, where Δ (0) is the zero temperature width and

Δ (T) is the width at arbitrary temperature [2].Figure (1-8) illustrates the relation between energy gap and critical temperature.
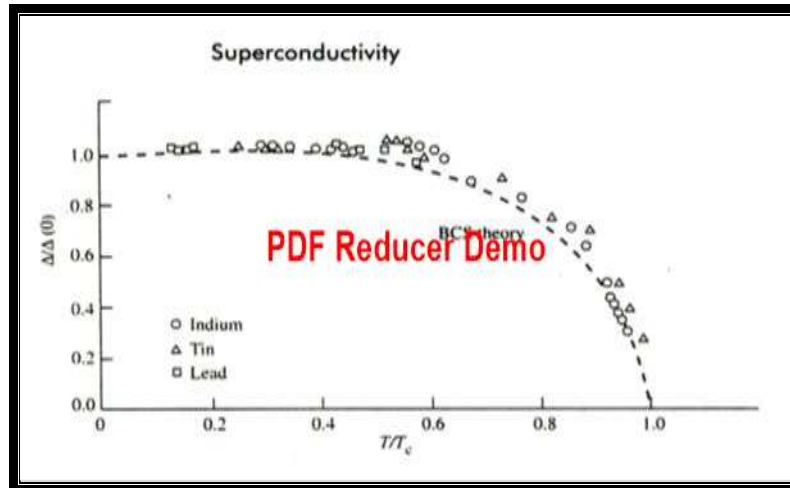
Figure(1- 8): Illustration of influence of energy gap in critical temperature [2].

1.12 Applications of superconductivity:

The discovery of superconducting materials with higher critical temperatures has led to the expansion of applications for superconducting materials. Some important applications for superconducting materials will be listed below:

1-The lack of loss of energy is superconductor led to the possibility of carrying a larger current in the winding, so it became possible to manufacture superconducting magnets smaller than resistive magnets [10].

2-Superconducting bulk can be used in water purification plants using the magnetic separation phenomena, so that more than 100 times the efficiency of purification can be obtained from the efficiency of the techniques currently used [39, 40].

16

3-Superconductors also utilized in designing of medical imaging systems, infrared sensors, microwaves devices and analog signal processing devices [41, 10].

4- Due to its high sensitivity to electric currents and magnetic fields, Josephson junction utilizes in manufacturing of interference quantum superconductor to employ it in the brain and heart activity detection [42, 43].

1.13 <u>Literature review:</u>

There are large numbers of research investigated preparation of BSCCO superconductor system due to its importance because it considered as one of the first superconductor compounds has T_c above 100k [44, 5].

Hazen *et al*. [1988] [45] recorded four superconducting Bi-Sr-Ca-Cu-O phases systems. The crystal structures of recorded systems were orthorhombic with unit cell dimension of about (5.41×5.44×30.78) ($\overset{o}{A}$)^3. The critical temperature of BSCCO systems were approximately 120k.

Yamada *et al*. [1988] [46] investigated the influence of Bi replacement by Pb on Bi-Sr-Ca-Cu-O superconducting system they noted that the T_c increased with increase of Pb concentration, the optimum result recorded was T_c=85.5k for $Bi_{1-x} Pb_x Sr_2CaCu_2O_\delta$ with (x=0.5) and more increase in Pb concentration produced negative results, where T_c decreased when Pb>0.5.

Li *et al*. [1989] [47] fabricated $Bi_{1.84}Pb_{0.34}Sr_{1..91}Ca_{2.03}Cu_{3.06}O_\delta$ superconducting system. They found that the fabricated specimens by solid state reaction have critical temperature of about 110k and XRD

analysis explained that the fabricated systems structure contained 2223 phase.

Dawud. [2000] [48] investigated the influence of n increasing on properties of HTSC, and also studied the influence of process of addition of 5% wt Lead (Pb) to the $Bi_2Sr_2Ca_{n-1}Cu_nO_{2n+4+\delta}$ compound which fabricated via solid state method Furthermore the free Pb specimens , the specimens sintered in $(845-848)^{o}C$ in oxygen environment. The results obtained indicated that PbO addition play positive role in critical temperature enhancement of fabricated BSCCO compound, where it had been found that the free Pb specimen has T_c approximately 105K and 130k for Pb-doped specimen. And also it had been found that increase of n up to 3.5 produced increase in T_c, but there is decrease in T_c associated to increase of n more than 4.

Hermiz. [2001] [49] investigated the influence of substitution concentration, sintering temperature, quenching, and oxygen content on $(Bi_{1-x}Pb_x)_2(Sr_{1-y}Ba_y)_2Ca_2Cu_3O_{10+\delta}$ fabricated system with substitution concentration (0>x>0.5) and (0<y<0.5) via using solid state reaction method. Results show that Tc=122K was the highest obtained critical temperature was for (x=0.2) and (y=0.1).

Zargar *et al*. [2008] [50] studied of bismuth (Bi) replacement by cadmium (Cd) and lead (Pb) on $Bi_{1.6}Pb_xCd_zSr_2Ca_2Cu_3O_y$ superconducting system with many substitution concentrations (x, z). The results explained that the increases in Cd concentration helped in Minimize the presence of not favorite's phases.

Kareem Ali Jassim [2005] [51] investigated influence of replacement of bismuth (Bi) by (Hg, Pb) and (Sr) by (Ba) on $(Bi_{2-x}(Pb,Hg)_xSr_{2-y}Ba_yCa_2Cu_3O_{10+\delta}$) superconducting system where

(x=0.1,0.2,0.25) and (y=0.1,0.2,0.25). XRD analysis explained that the change in the replacement (Sr, Ba and Hg) produced change in density, c/a ratio and ratio of high phase (Bi-2223). The electrical resistivity tests explained that the critical temperature were (T_c=125,129,119K) for ($Bi_{1.75}Pb_{0.25}Sr_{1.9}Ba_{0.1}Ca_2Cu_3O_{10.26}$), ($Bi_{1.75}Hg_{0.25}Sr_{1.9}$ $Ba_{0.1}Ca_2Cu_3O_{10.271}$) and ($Hg_{0.75}Pb_{0.25}Sr_{1.75}$ $Ba_{0.25}Ca_2Cu_3O_{8.31}$) respectively .

Hayder Jawad Maktoof [2005] [52] investigated Pb partial substitution influence on structural and electrical properties of $Bi_{2-x}Pb_xSr_2Ca_2Cu_3O_{10}$ HTSC system which fabricated via solid state reaction , where (x=0, 0.1, 0.2, 0.3 and 0.4). XRD analysis explained that the prepared specimens have orthorhombic crystal structure and there are three phases were found (2201,2212 and 2223). The optimum magnitude of critical temperature was T_c=123k for x=0.4

Majeed Ali Habeeb [2006] [53] investigated the influence of partial substitution of (Bi) by (Pb) and (Sr) by (Ba, Sb) on $Bi_{2-x}Pb_xSr_{2-y}(Ba,Sb)_yCa_2Cu_3O_{10}$ system which fabricated via solid state reaction method, where (0.6≤x≤1) and (0≤y≤0.5). XRD analysis explained that

the prepared specimens have orthorhombic crystal structure with presence of two superconducting phases (2212 and 2223) in addition to other phases. The resistivity measurements results explained that the increase of Ba substitution concentration produced increase T_c, but increase of Sb and Pb substitution concentration produce decrease in T_c, where the best magnitude of T_c =119k for (x=0.6) , while the specimens transform to semiconductors or insulators at increase Ba and Sb concentrations (0.4 and 0.5) and (0.2 and 0.3) respectively.

Thabitt *et al*. [2011] [54] investigated Cu by Ni partial replacement influence on $((Bi_{0.8}Pb_{0.2})_2(Sr_{0.9}Ba_{0.1})_2Ca_2Cu_{3-x}Ni_xO_{10+\delta})$

19

superconducting system, where (x=0, 0.1... 1, 2, 3). They found the highest T_c can obtained was 113k associated to x=0.8. XRD analysis explained that the crystal structure of specimens is orthorhombic with decrease in length of C-axis corresponding to Ni concentration increase.

Bilgili *et.al.* [2012] [55]. investigated Nb addition influence on properties of $Bi_{1.7-x}Pb_{0.3}Nb_xSr_2Ca_2Cu_3O_y$ superconductor system where (x= 0.00, 0.05, 0.1, 0.15 and 0.2). After they fabricated the specimens utilizing SSR technique, they found that the best substitution concentration was (0.2), where XRD patterns illustrated that there was increase in high temperature phases volume fraction$V_{ph-2223}$, where $V_{ph-2223}$=0.86 at x=0.2.

Halim *et.al.* [2012] [56] investigated influence of (MgB_2) addition on properties of $(Bi_{1.6}Pb_{0.4}Sr_2Ca_2Cu_3O_\sigma)$1-x (Mg$B_2$)x superconductors system synthesized via SSR technique, where (x= 0.00, 0.002, 0.004, 0.006, 0.008 and 0.010). They found that volume fraction of high temperature phase diminished from 85% to 25% when (MgB_2) ratio raised, and also found that there is larger grains and pours structure ware observed after add (MgB_2), coupling loss was explained by the complex susceptibility measurement.

S.M.Shaban *et.al.* [2013] [57] investigated influence of Bi by Cu and Pb partial replacement on insulating properties behavior of (real and imaginary parts of dielectric constant, tanδ and alternative conductivity) of (Bi$_{2-x}$(CuPb)$_x$Sr$_2$Ca$_2$Cu$_3$O$_{10+\delta}$) superconductor system at room temperature which fabricated via solid state reaction method, where (x=0,0.4and0.5) . The results explained that the dielectric constant attributed to phase transitions. They also noted there is increase in value

of tanδ with frwquency and x. Alternative current exhibited increase with frequency increase to each value of x.

Bushra A. W. Aljuran[2007] [48] [10], investigated influence of fast neutron and thermal neutron irradiation on *$Hg_{1-x-y}Tl_xPb_yBa_2Ca_2Cu_3O_{8+\delta}$* superconductor systems properties, she utilized from ^{241}Am/Be source has 5MeV average energy 2.8×104 n/ cm^2.sec, she found that phase transformation from tetragonal to orthorhombic happened due to specimens exposed to fast neutron irradiation and decreases in critical temperature was detected. The same source was utilizing to thermal neutron irradiation process with average energy about of 0.025eV and flux of 4.62×10^2 n/ cm^2.s, she observed that there were increases and decreases in critical temperatures T_c of specimens, but there was not phase transformation happened after irradiated by thermal neutron.

Kareem Ali Jassim *et. al.* [2013] [58], studied the influence of neutron irradiation on the properties of $Tl_{0.6}Pb_{0.3}Cd_{0.1}Ba_2Ca_2Cu_3O_\delta$ superconductors system which was fabricated by solid state reaction technique, specimen A prepared without irradiation, but B,C and D exposed to neutron irradiation of a dose about 6.04×10^{10}, 12.08×10^{10} *and* 18.12×10^{10} n/cm^2respectively by utilizing$^{241}Am - {}^9Be$ source . They found that the critical transition temperature $T_{c(offset)}$ decease with dose increasing from 166K to 113K, 112K, 111K respectively. They also observed by XRD that the fabricated specimens contain major pure-phase polycrystalline Ti (Pb,Cd)-1223 and little amount of (Ti -1212), and specimen A has higher intensity than specimens B,C and D. Lattice parameter a and c, c/a ratio and volume fraction all exhibited decrease with increasing dose irradiation .

Nour abdul-wahid[2015]. [59]investigated influence of laser ray on properties of $TI_{2-x}Hg_xBa_{2-y}Sr_yCa_2Cu_3O_{10+\delta}$ superconductor system, she observed from XRD patterns of specimens before and after exposed to laser ray that some of specimens exhibited decrease in theirs c-axis length values while the another exhibited increases in theirs c-axis length, on the other hand, she observed that the critical temperature of specimens before and after exposed to laser ray exhibited decreases for some specimens but another specimens exhibited increases in theirs critical temperature.

1.14 Aim of the work:

The initiation of this work is attributed to two reasons, the first reason is to try to improve properties of $Bi_{2-x}Pb_xSr_2Ca_nCu_{n-y}Ni_yO_{2n+4+\delta}$ superconductor system with (n=2 and 3) by partial substitution of Bi by Pb and Cu by Ni with different substitution concentration (x, y). The second reason is to know the effect of different categories of radiation on the compound that has been prepared, this reason is divided into two sub-cause, namely, the attempt to improve the characteristics of the compound that was prepared, the second sub-cause is to provide sufficient information about the negative consequences that may result from the expose of the compound, it was prepared for various categories of radiation (fast neutron radiation, laser radiation and beta particle radiation). The second sub-cause is the fact that some superconducting materials are applied in some devices that make them susceptible to different types of radiation, providing information about the fate of superconducting materials exposed to radiation, and causing damage. That will enable designers to overcome these problems by shielding the superconducting parts to resist the type of radiation exposed to it, or design the device in appropriate ways to maintain the superconducting

parts of the radiation beam to maintain its efficiency, especially that since the efficiency of superconductors is related to the working temperature (critical temperature) and any drop in the temperature at which the superconductor works is considered a loss of the efficiency of the performance of the device.

Chapter Two

High temperature superconductor

Chapter two
High temperature superconductor

2.1 <u>Introduction:</u>

The most important property of high temperature superconductor HTS substances that its Tc magnitude highest than boiling point of liquid nitrogen (77K). The chemical compounds of these substances contains regular repeated manner of several elements atoms, defined as unit cells. The way by which the HTS was manufactured play important role in limit the utilization of HTS, it is suitable for utilize in electrical products [5, 60]. In 1988 , Maeda explored Bi-Sr-Ca-Cu-O (BSCCO) superconductor system with chemical formula $Bi_2Sr_2Ca_{n-1}Cu_nO_{2n+4+\delta}$ [35, 61].

2.2 <u>Crystal structure of (BSCCO):</u>

The chemical formula of BSCCO compound is $Bi_2Sr_2Ca_{n-1}Cu_nO_x$, where n defined as the copper layers number and take the value n= 1 , 2 , 3. Thus there are three phases of BSCCO [53, 62], the first phase is $Bi_2Sr_2Cu\,O_{6+\delta}$, it is popularly known as 2201 phase and has critical temperature about 10-20K [63] be conditional on oxygen content ,so it was categorized as very low temperature phase, in this system there is only one CuO_2 layer. The second phase is $Bi_2Sr_2Ca\,Ca_2O_{8+\delta}$ is popularly known as 2212 has critical temperature about 50-95K also be conditional on oxygen content , there is one layer of Ca between two CuO_2 layers in this phase . The third phase (n=3) is $Bi_2Sr_2Ca_2Cu_3O_{10+\delta}$, it is popularly known as 2223 phase has critical temperature about 110k , there is weak dependence on oxygen content , in this phase there are two Ca layers between three CuO_2 layers as demonstrated in figure(2-1). The x-ray diffraction explain that the standard lattice parameters have a magnitudes of a=5.383Å, b=5.376 Å, and c=24.38Å for 2201 phase

(single crystal), and a=5.395 Å , b=5.390 Å, and c=30.65 Å for the 2212 phase(single crystal) , and a=b=5.4 Å and c=37 Å for the 2223 phase (polycrystalline). But these magnitudes can vary depending on cation substitution [64, 65].
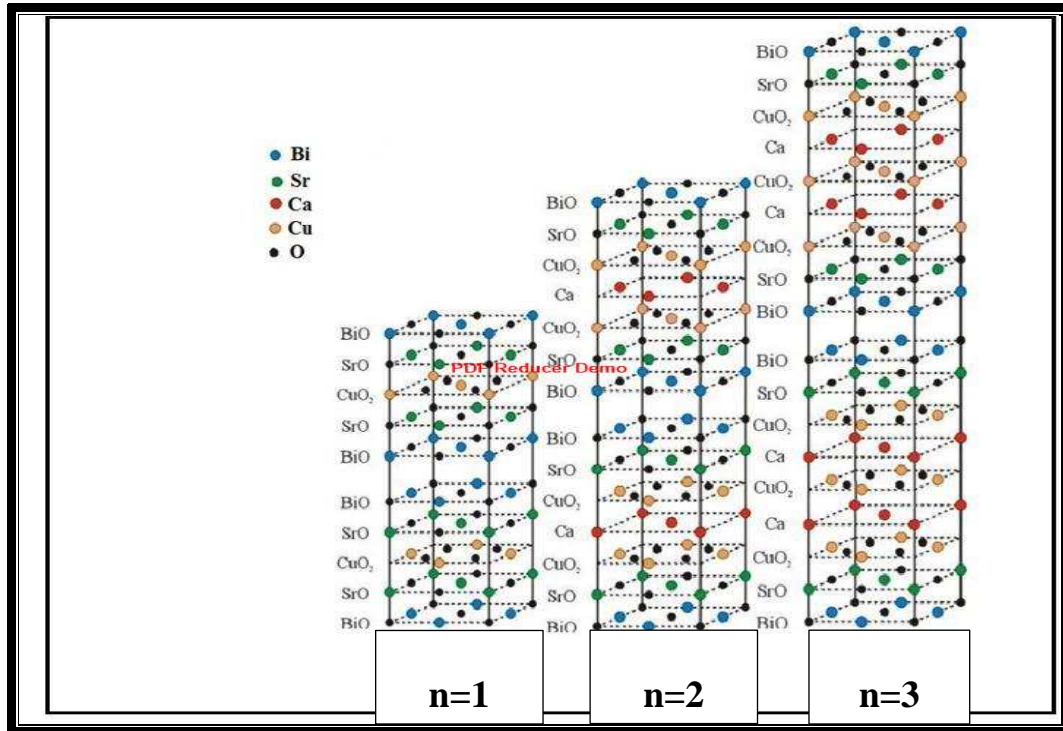
Figure2- 1 :Crystal structure of (BSCCO) phases [66].

2.3 **Perovskite composition:**

The high temperature superconductors were explored in perovskite compounds, this ceramic compounds compose from joining of metallic substances which represent cat ions with non-metallic substances which represent anions such as oxygen. The general form of Perovskite compounds is ABX_3, the metallic substance involves positive charges A and B cat ions, where A –cat ion has large volume and located in the center of cube but B-cat ion has small volume and located in each of cube eight corners. The non-metallic substances involve negative anions which have small volume and located on the half of each sides of cube (between two B-cat ions) [67, 1]. The Perovskite usually serve as insulator and

25

their atomic structure and atomic orbits are filled. Most Perovskite compounds are deformed when A-cat ion is smaller than B–cat ion, so crystal structure inclination may be introduces in the unit cell. The negative electrons being on one side and the positive charges being on the other side causing strong polarization. This polarization play important role in explanation of superconductivity phenomena as demonstrated in Figure (2-2).
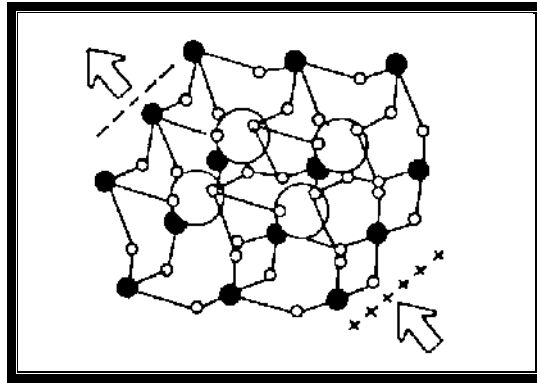
Figure2- 2: Crystal polarization [1].

2.4 The high temperature superconductors theories:

2.4.1 Interlayer model:

There are a lot of compounds consist of CuO_2 layers in their structure, the copper-oxide layers in these compounds are sandwiched around different elements layers. The charge carriers (electrons or holes) are considered to establish essentially with in copper oxide layers [68, 69]. The movements of superconducting current take place between two CuO_2 layers normal to c-axis direction. The distance between two copper oxide layers is ($d_{Cu-Cu}12.1A^{\circ}$) this distance larger than the coherence length (ξ=4A°) but ξ approximate to magnitude of the distance from BiO

layer (d_{M-Cu} =4.4 A^{o}). Therefore the super current can translate between CuO_2 layers only by tunneling through the metallic layers [70, 43, 71].

2.4.2   Exition model:

Based on this model, the affective attraction between the electrons occurs by the exition and not as known by the phonons, and it was suggested that there are two conduction bands. Allander suggested the Exition model to understand superconductivity at high temperatures. He suggested that if the metal was placed in direct contact with a polarized semiconductor then the metal electrons would react with the inter band excitation of the semiconductor. As a result of the exchange in these effective excitation the electron pairing will take place .And certainly, this will weaken Coulomb's repulsion of the electrons [72, 73].

2.4.3 Plasmon model:

The Plasmon was known as a description of collective vibration of carriers interest to the lattice. Branch of Plasmon called demon, the numbers of demons increase in the state of more energy band overlapping. In the case of existence of double band, this mean there are double carriers category classified as light and heavy carriers, these two categories oscillate simultaneously depending on each other [72]. In the same way by which the phonons exchange, the demons will exchange, thus the light carriers came from pairs. The attraction created by Plasmon and ordinary repulsion produce electron-electron interaction.

2.4.4 Oxygen defect model:

Based on this model, the pairing interaction was improved by combination that takes place between oxygen defects certain structure and electron of copper pairs, these oxygen defect was suggested to be

existence with arbitrary distribution in Cu-O_2 layers of HSC [35, 74]. One electron strongly pule electrons toward copper ions pairs . at this position , there is big probability to finding the electrons between two ions with singlet spin connection .There are a lot of phenomena have been recorded involve spin glass-like manner support and assure the relation between oxygen content and superconductor properties. For this reason attributed the short positron lifetime in superconductors [51, 75]

2.5 **Neutron radiation:**

The most important characteristic of neutron radiation is that it does not lose its energy when interacting with electrons, unlike the reaction of electron radiation with electron, so when superconductor specimens exposed to neutron radiation there is no loss in neutron energy during interaction between neutrons and electrons of specimens atoms shell. The neutron- electron elastic interaction causes atoms shifting from their original locations in the crystal lattice .when inelastic collision causes transmitted of enough energy to the primary atoms the point defect will produce , and some of defect was formed from agglomeration of point defects because of the knock on movement of secondary subsequent atoms will take place [72, 76]. The spherical defect of about 5-6 nm will generate because of vacancy domain around agglomerated defects [77, 72]. There is the homogeneity in distribution of defect because of high penetrating power of neutron radiation [78, 72] , but this high power of penetration make the neutrons radiation weak in the interaction , that is mean needing high dos or long time of neutron

Irradiation [79, 72].

2.6 Beta radiation:

There are three mechanisms by which the interaction between beta particles and matter occurs: the first mechanism is the excitation of electron orbital, in this state the kinetic energy of beta particles is dissipated. The second mechanism is the ionization which defined as the phenomena by which the atom or molecular lose electron to produce positive ion or gain electron to produce negative ion, and the third mechanism called Bremsstrahlung production which defined as dissipation of radiative energy [80].

2.7 Laser radiation:

Due to its ability to change the properties of substance which exposed to its ray, laser radiation utilize under controlled condition. The absorption happen during irradiation lead to interaction produce between laser ray and substance, It is also possible to get interaction by excitation due to high intensity of laser ray. Thus there are electronic and thermal events associated to irradiation of substance utilizing laser ray [81].

Chapter Three

Experimental work

Chapter three

Experimental work

3.1 <u>Introduction:</u>

This chapter involves explanation of fabrication methods of Bi_{2-x} $Pb_X Sr_2 Ca_{n-1} Cu_{n-y} Ni_y O_{2n+4+\delta}$ compound with(n=2 and 3) (x=y=0, 0.2 and 0.4), and also involves explanation of measurement ways that was utilized to investigate several properties like x-ray diffraction (XRD), measurement of   electrical resistivity as a function of absolute temperature and Determination of Oxygen Content. The work was divided into four steps:

1- Materials preparation step.

2- Specimens fabrication step

3- Specimens irradiation step.

4- Tests and measurements step**.**

3.2 <u>Powders preparation:</u>

The high purity oxide materials were utilized to fabricate (BSCCO) system, they involve ($Bi_2 O_3$, $Pb_3 O_4$, CaO ,CuO and $Ni_2 O_3$), expect strontium oxide(SrO) was obtained from strontium nitride (Sr$(No_3)_2$) after making experimental attempts of heat treatments, the best result was by putting (Sr$(No_3)_2$) inside furnace with $900 C^\circ$ for 48 hours with rising rate(10 C°/min). XRD technique was utilized to insure from the strontium oxide produced after heat treatment by comparing with standard card which Issued by International Center for Diffraction data (ICDD)and has a serial number (00-048-1477 SrO) as illustrated in figure (3-1):
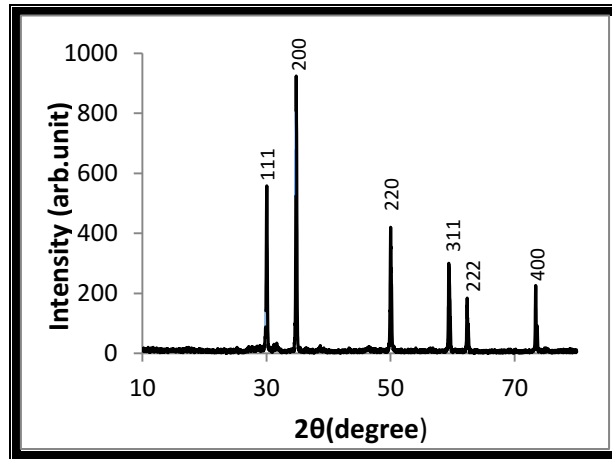
Figure3- 1:XRD pattern of obtained strontium oxide(SrO).

3.3 Specimen's fabrication:

Conventional solid state reaction method was utilized in specimens preparation , the first sub step in this step is mass required calculation by use the following equation :$(2 - X)/2\ Bi_2O_3$ +(X/3) Pb_3O_4 +2SrO+(n-1)CaO+(n-y)CuO+(y/2)$Ni_2O_3 \rightarrow Bi_{2-x}\ Pb_X\ Sr_2\ Ca_{n-1}\ Cu_{n-y}\ Ni_y\ O_{2n+4+\delta}$.

The molecular weight of each element was utilized to calculate the mass of each material required as listed in the table (3-1):

Table3- 1: Atomic weight of utilized powders.

Powder material	Atomic Weight ratio
Bi_2O_3	(2-X)/2 [2 (208.9804)+3(15.9994)]
Pb_3O_4	X/3[3*(207.02)+4*(15.9994)]
SrO	2[87.62+15.9994]
CaO	n-1[40.078+15.9994]
CuO	(n-y)[63.546+15.9994]
Ni_2O_3	y/2[2*(58.693)+3*(15.9994)]

After calculating the required powder mass, a suitable quantity of oxides powder of each material of Bi_2O_3, Pb_3O_4, SrO , CaO, CuO and Ni_2O_3 was dried utilizing oven under $100C^{\circ}$ for 1 hour to elimination of

31

moisture, and then the sensitive balance with four digits model (KERN) was utilized weighting the needed quantities of powders.

The powders mixed together with 2-propanol and grinded utilizing agate mortar for 30 min, and then mixed again by utilize of vortex mixer for 2 hours to ensure a mixture of homogenized powder and dried again. The produced powder mixture pressed in form of cylindrical pellets that have diameter 1.5 cm and 0.2 cm thickness by utilize of hydraulic press under pressure of 7 ton/cm^2 (3.56 MPa).

The last step in specimens fabrication is sintering of green pressed pellets by utilize of furnace at $800C^{o}$ for 120 hour with rate of heating 5 C^{o}/min under normal atmospheric pressure and then the temperature decreased to room temperature with rate 5 C^{o}/min.

3.4 <u>Specimens fast neutron irradiation:</u>

The fabricated specimens were irradiated by fast neutron irradiation utilizing thermal neutron source $^{241}Am/Be$ with neutron flux 10^5 neutron/$cm^2.sec$ and energy of 5 MeV for 15 days i.e. (1.296$\times 10^{11}$ n/cm^2). The specimens were pasted onto a tape after covering them with labeled paper and turned around a cadmium ring, then putting this ring around the source of neutron. The covered specimens and neutron source box illustrated in Figure(3-2)
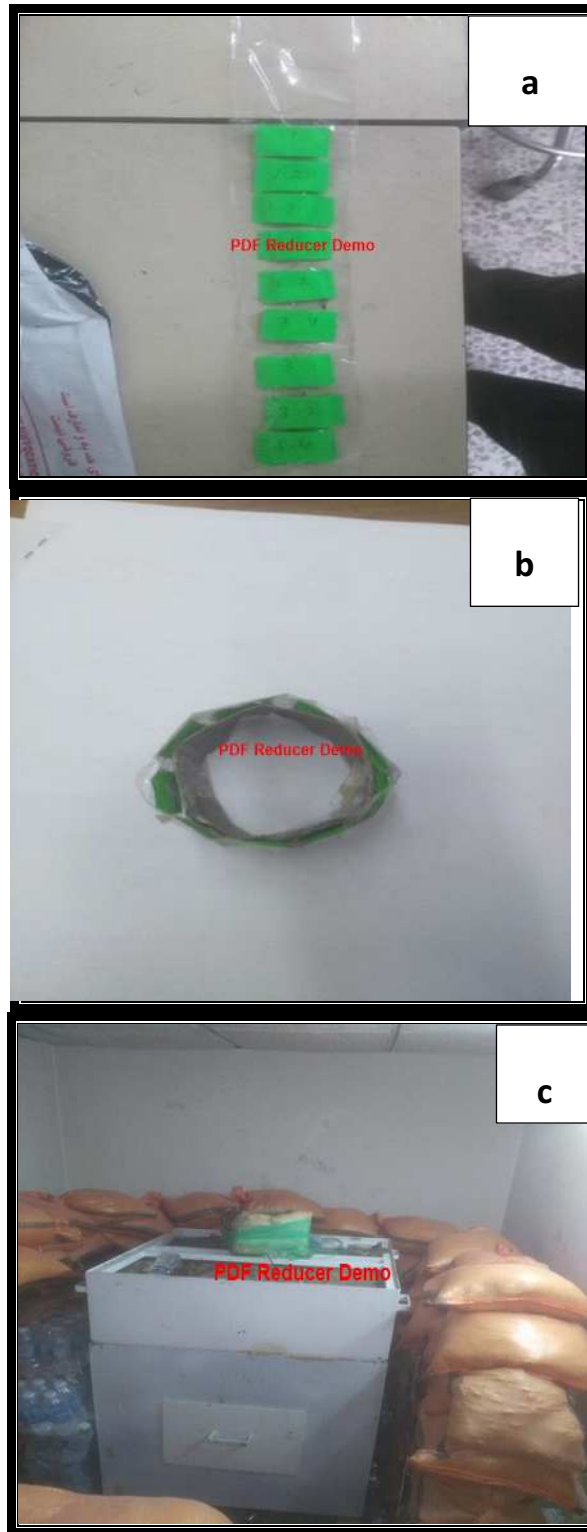
Figure3- 2:Specimens fast neutron irradiation

(a)Specimens taped and labled.

(b)Specimens turned around cadmium ring.

(c)Fast neutron source box.

3.5 <u>Specimens diode- laser irradiation:</u>

The fabricated specimens were exposed to laser irradiation by utilize of diode-laser source (red laser dot module focusable) has output power 150 mW and wavelength of 650 nm. The specimens were placed 15 cm away from the laser source, and one hour time for each specimen. Figure (3-3) represent real picture of utilized laser source.

Figure3- 3: Specimen laser irradiation.

34

3.6 **Specimens Beta irradiation:**

The fabricated specimens exposed to beta particles irradiation utilize of $^{90}Sr/^{90}y$,β^-plane source with activity of 0.75 Ci and dose rate of $2.648*10^4$Gy/hr. The specimens pasted onto tape after covered by paper as illustrated in Figure(3-4) placed apart 15cm of a source for 14 days i.e. the dose was $887.08*10^8$ Gy.

Figure3- 4: specimen taped and labeld to subjected to beta irradiation

3.7 **Tests and measurements:**

3.7.1 **X-ray diffraction test:**

x-ray diffraction analysis was utilized to investigate the crystal structure of fabricated specimen was type (Shimadzu) has $Cu_{k\alpha}$ source with 40 kv supplied voltage, 30 mA current, $1.5406A^°$wavelength and 10-80 degree diffraction angle range at the room temperature. The magnitude of I (arbitrary unit) and 2θ (degree) that brought from the results data was compared with standard cards to find miller indices (hkl)

magnitude and determine the composed phases. The planes distance d was calculated utilizing brag law:

nλ=2d sinθ ……………………..(3-1)

Where n: The integer number, λ: The sources wave length (angstrom unit) , d:The distance separates the crystalline planes(angstrom unit) , θ: The angle was located between the incident beam and diffracted beam(degree unit).

The lattice parameter a,b and c was calculated utilized the equation [3-2] by using computer program based on Cohen's least square method [81].

$$\frac{1}{d^2} = \frac{h^2}{a^2} + \frac{k^2}{b^2} + \frac{l^2}{c^2}$$ ……………..(3-2)

The volume fraction for each phase was estimated utilizing the following equation [35].

$$v_{ph} = \frac{\sum I_c}{\sum I_1 + \sum I_2 + \sum I_n} \times 100\%............(3-3)$$

Deby sherrer equation was utilized to estimate crystallite size:

$$\tau = \frac{k\lambda}{d\,cos\theta}$$…………………………....(3-4)

Where: τ is a crystallite size (nm), K is a constant, λ is a wave length, θ is an diffraction angle, d full width half maximum (F.W.H.M)(degree unit).

3.7.2 :Resistivity as a function of temperature measurement:

Four – probes technique was utilized to calculate the resistivity as a function of absolute temperature and determine the temperature at which the resistivity decreased to zero magnitude which usually called critical temperature (T_c). This technique involve several parts , the four – probes involve outer two probes connect to direct current supplier while the inner two probes connect to Nano voltmeter the four probes get a touch

with specimen via silver paste . The four probes were installed inside the cryostat, this cryostat was connected to router pump to make the pressure inside it approximately equal $(6 \times 10^{-2} \text{mbar})$, and also jointed to thermocouple type-K to measure the temperature of the specimen surrounding. Figure (3-5) and (3-6) represent four probes test diagram and real image respectively.
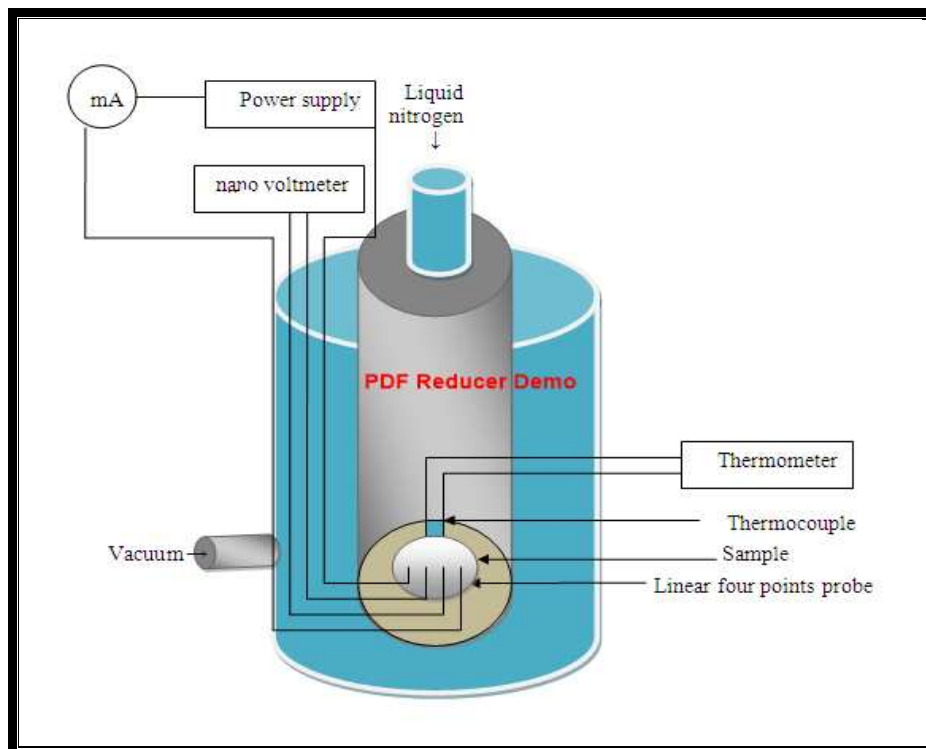

Figure3- 5: Four-probes test diagram.

Figure3- 6:Real image of four probes test.

Liquid nitrogen was added to cryostat to decrease its temperature to 77K and measure the voltage as a function of temperature. The resistivity of each temperature was calculated from the magnitude of voltage at each temperature with aid of relation [5].

$$\rho = \frac{V}{I} \frac{Wt}{L} \dots\dots\dots\dots\dots\dots\dots\dots\dots \quad (3\text{-}5)$$

Where: **I** is the current carried along the specimen (mA), **V** is the measured voltage between electrodes (mV), **t** is the pellet thickness (Cm), **L** is the length of pellet (Cm), **W** is the pellet width (Cm).

Since all specimens have constant calculated thickness, length and width, hence the relation (3-5) can express as:

$$\rho = 4.5324 \frac{V}{I} \dots\dots\dots\dots\dots\dots\dots(3\text{-}6)$$

The estimation of the critical temperature of transition Tc depends on the curve which represents the relation between the resistivity and absolute temperature as illustrated in Figure (3-7).
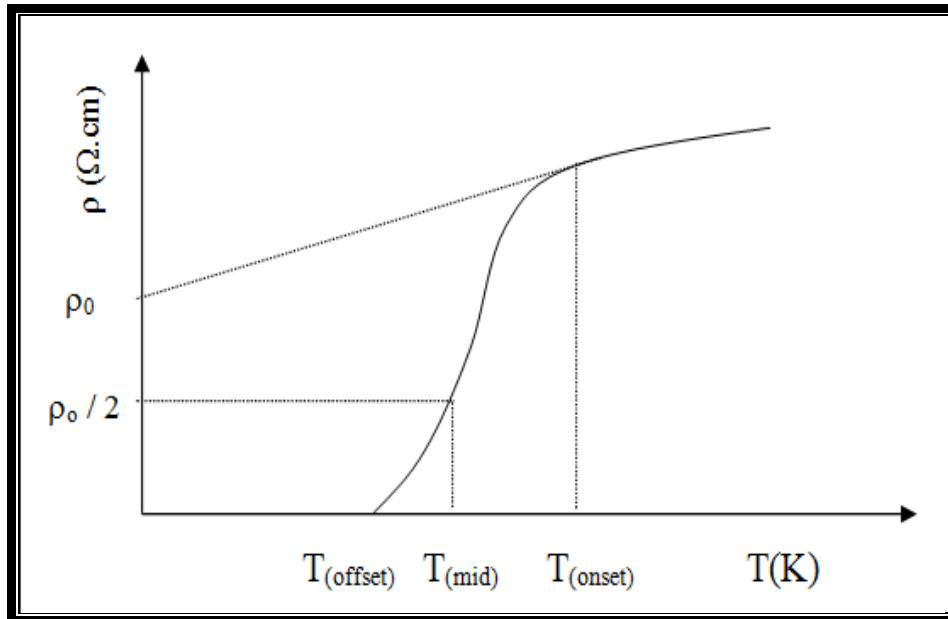
Figure3- 7: The curve was utilized to determine midpoint of Tc.

The midpoint T_c was calculated from relation (3-7) [35].

$$T_{c(mid)} = \frac{T_{C(offset)} + T_{C(onset)}}{2} \quad \ldots\ldots\ldots(3\text{-}7)$$

Where: $T_{C(onset)}$ is the initial critical temperature, $T_{C(offset)}$ is the temperature at $(\rho = 0)$ [35].

3.7.3 Estimation of oxygen content:

The oxygen content of fabricated specimens before and after expose to different categories of radiations were estimated utilizing traditional chemical method called titration; this method was implemented as follows:

1- Take the amount of (45 mg) of the sample to calculate the level of oxygen and to be grinded in an agate mortar.

2- Dissolve 3.17g of potassium iodide (KI) in 2.5 ml of distilled water.

3- Place the sample powder in a beaker and pour 2.5ml of potassium iodide (KI) solution in addition to 1.25 mL of hydrochloric acid HCL with a concentration of 10%, then Mix the powder with these

two solutions well by place the beaker on a Magnetic stirrer and put a magnetic bar inside the beaker until it turns dark brown to a proof of iodine I_2 release.

4- Dissolve 0.3g of sodium thiosulfate ($Na_2S_2O_3$) in 20 ml of distilled water to obtain concentration of approximately (0.015 gm./ml) and put it in a glass burette which set up above the beaker, then add drops of sodium thiosulfate solution to the beaker until it turns to light brown.

5- Dissolve 10g of starch in 100 ml of distilled water and add this starch solution ($C_6H_{10}O_5$) to the beaker until the mixture becomes dark blue.

6- Add sodium thiosulfate solution drops again but slowly until the solution turns yellow. This is evidence of complete reaction.

7- Calculation of the volume(V) of the sodium thiosulfate solution used in the reaction and insert (V) value in the following equation [1]:

$$\delta = \frac{\left[\frac{M_A}{M_B}\right] - \left[\frac{3m_A}{CV}\right]}{\left[\frac{2m_A}{CV}\right] - \left[\frac{M_\circ}{M_B}\right]} \quad \ldots\ldots\ldots\ldots\ldots\ldots(3\text{-}8)$$

M_A is Molecular weight of the sample compound to calculate its oxygen content (g / mole), M_B:molecular weight of sodium thiosulfate solution ($Na_2S_2O_3$) is equal to M_B= 248.18 g / mole, m_A: The sample mass used in the correction process is equal to m_A = 45 mg, **C**: the concentration of sodium thiosulfate solution is equal to **C** = 0.015 g / ml, **V**: The volume of sodium thiosulfate solution used in the correction process (ml), $M_\circ$: Atomic weight of oxygen is equal to $M_\circ$ = 15.999 g / mole.

Chapter four

Results and discussion

Chapter Four
Results and discussion

4.1 <u>Introduction:</u>

This chapter includes properties description of prepared specimens of $Bi_{2-x}Pb_xSr_2Ca_2Cu_{3-y}Ni_yO_{2n+4+\delta}$ system which has two phases n=2 (2212) and n=3 (2223) with substitution concentrations (x =y= 0, 0.2 and 0.4). X-ray diffraction analysis, Iodometric titration, and electric resistivity were studied to determine the best concentration of substitution and to investigate the influence of different categories of irradiation on prepared specimens.

4.2 <u>X-ray diffraction analysis results:</u>

4.2.1 <u>Influence of Pb and Ni substitution on structure properties of (BSCCO)</u>

X-ray diffraction pattern of $Bi_{2-x}Pb_xSr_2Ca\,Cu_{2-y}Ni_yO_{2n+4+\delta}$ specimens with substitution concentrations (x=y=0, 0.2and 0.4) was illustrated in figure (4-1). It has been observed that all specimens patterns have multiphase include major high- T_c phase 2212 (H-peaks) and minor high-T_c phase 2201 (L-peaks) with orthorhombic crystal structure system. Clearly there is an increase in peaks intensity associated with increased concentration of substitution. Software program based on Cohen's least square method [82] was used to compute lattice parameters a, b and c. The computed magnitudes of lattice parameters were listed in tables (4-1), it is noticeable that the c-axis length increased and a-axis and b-axis decreased with increase of substitution concentrations, this change in lattice parameters attributed to the difference in ionic radius between

$(Pb^{+2}=1.2\ A^{\circ})$ and $(Bi^{+3}=0.9\ A^{\circ})$ [53]and also between $(Ni^{+3}=0.78\ A^{\circ})$ and $(Cu^{+2}=0.96A^{\circ})$ [54]. Figure (4-2) illustrated the relation between c and substitution concentration. The difference between substituted ionic radius and that of original ions produce reducing in unit cell volume, so the mass density was increased as listed in Table (1-1). Volume fraction v_{2212} value increased with substitution concentration increase as listed in table and demonstrated in figure (1-1).
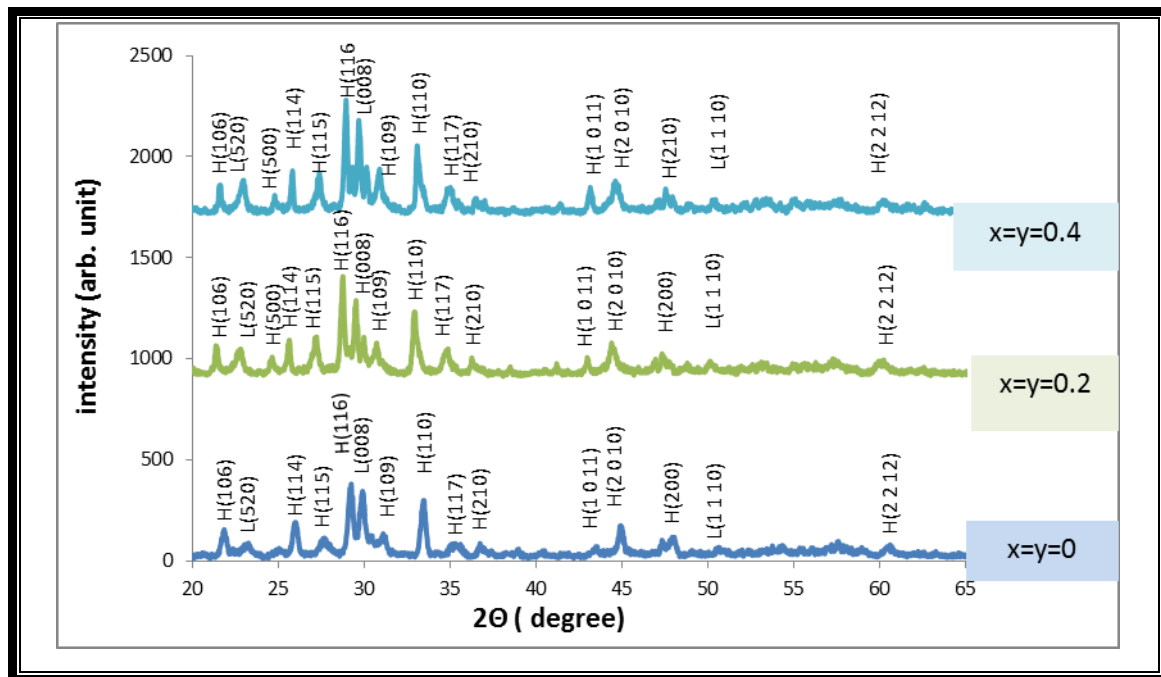

Figure4- 1:XRD pattern of $Bi_{2-x}Pb_xSr_2Ca\ Cu_{2-y}Ni_yO_{8+\delta}$**specimens (x=y=0,0.2, 0.4).**

Table4- 1:magnitudes of a,b,c,c/a ratio,mass density,v2212, v2201 and crystal size of $Bi_{2-x}Pb_xSr_2Ca\ Cu_{2-y}Ni_yO_{2n+4+\delta}$ **specime with substitution concentrations (x=y=0, 0.2 and 0.4).**

Specimen	a (A°)	b (A°)	C (A°)	c/a	volume $(A^{\circ})^3$	ρ_m g/ cm^3	V_{ph} 2212	V_{ph} 2201	Crys. size (nm)
$Bi_2Sr_2Ca\ Cu_2O_{8+\delta}$	5.387	5.459	30.97	5.74	910.754	1.617	78%	21.7%	35.56
$Bi_{1.8}Pb_{0.2}Sr_2Ca\ Cu_{1.8}Ni_{0.2}O_{8+\delta}$	5.38	5.427	31.104	5.78	908.1515	1.623	79.2%	20.4%	32.21
$Bi_{1.6}Pb_{0.4}Sr_2Ca\ Cu_{1.6}Ni_{0.4}O_{8+\delta}$	5.375	5.406	31.133	5.79	904.639	1.625	79.3%	20.1%	31.37
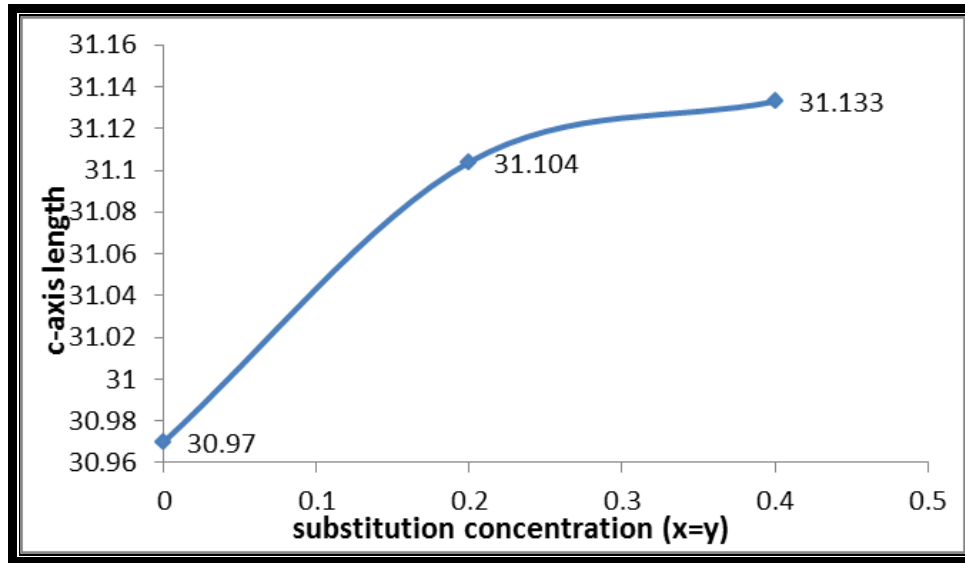
Figure4- 2:The relation between substitution concentration and c-axis of $Bi_{2-x}Pb_xSr_2Ca\ Cu_{2-y}Ni_yO_{2n+4+\delta}$.**specimens.**

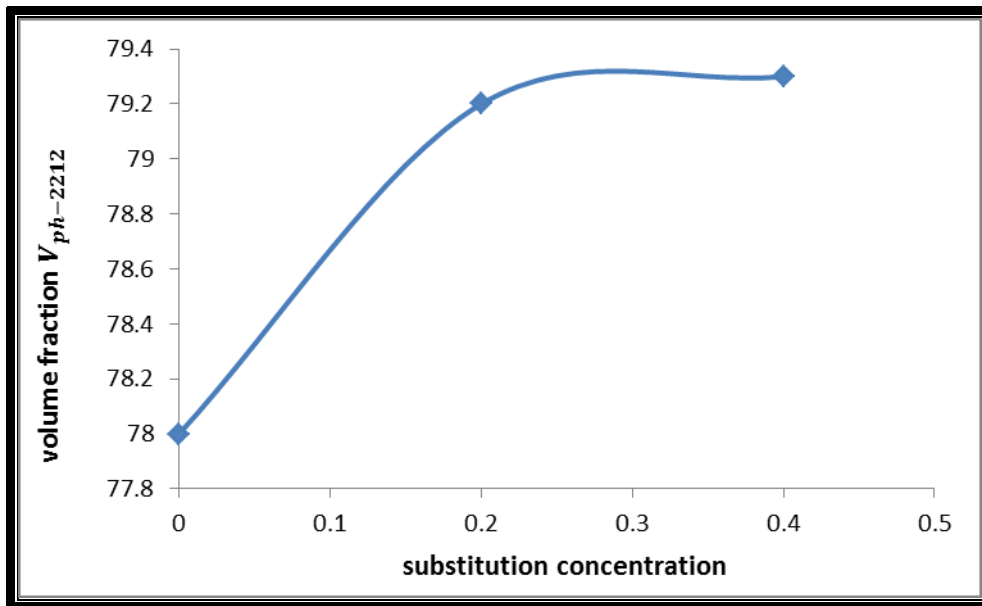**Figure4- 3:The relation between volume fraction** $(V_{ph-2212})$**and substitution concentration of** $Bi_{2-x}Pb_xSr_2Ca\ Cu_{2-y}Ni_yO_{2n+4+\delta}$. **Specimens.**

X-ray diffraction pattern of $Bi_{2-x}Pb_xSr_2Ca_2\ Cu_{3-y}Ni_yO_{2n+4+\delta}$ specimens with substitution concentrations (x=y=0, 0.2and 0.4) was illustrated in Figure (4-4). It has been observed that all specimens patterns have multiphase include major high- T_c phase 2223 (H-peaks) and minor low-T_c phase 2212 (L- peaks), evidently there is an increase in peaks intensities after substitution. The estimated lattice parameters magnitudes

were listed in Tables (4-2). It is noticeable that the c-axis length increased but a-axis and b-axis decreased with increasing of substitution concentrations. This change in lattice parameters attributed to the same reason of $Bi_{2-x}Pb_xSr_2Ca\,Cu_{2-y}Ni_yO_{2n+4+\delta}$ specimens which above-mentioned, thus the volume of unit cells decreased, this decrease produce increase in density as listed in Table (4-2). Figure (4-5) explained the relation between c and substitution concentration. The volume fraction of H-peaks ($V_{ph-2223}$) also listed in Table (4-2), it has been observed that ($V_{ph-2223}$) increase with increasing of substitution concentrations as demonstrated in figure (4-6).
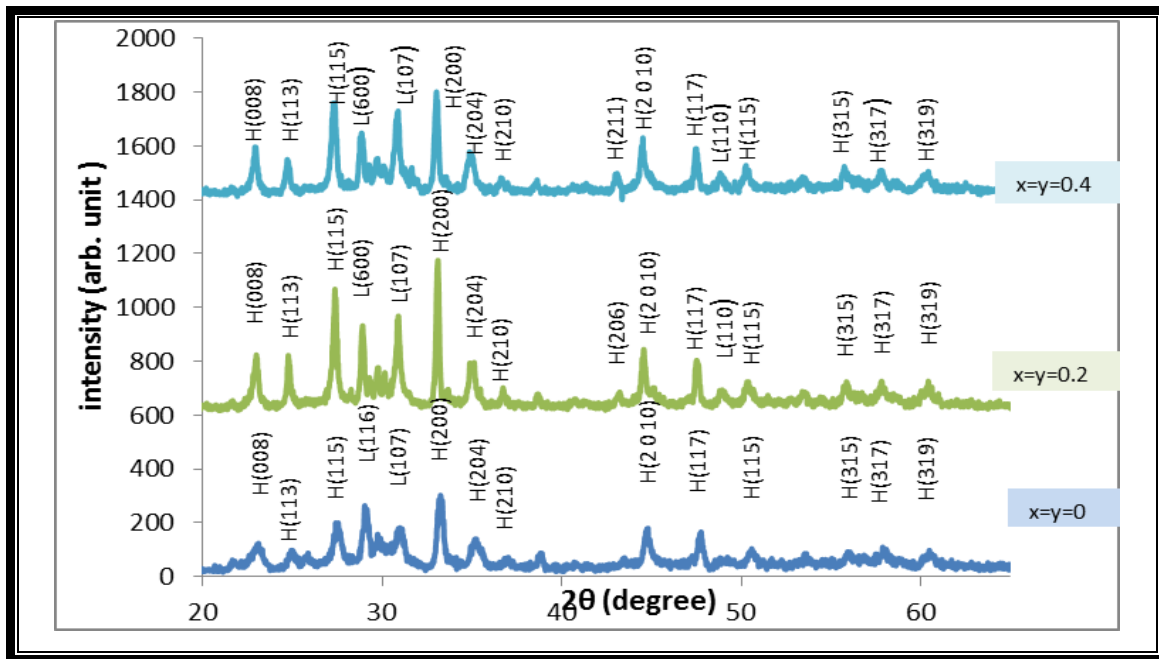

Figure4- 4:XRD pattern of $Bi_{2-x}Pb_xSr_2Ca_2Cu_{3-y}Ni_yO_{8+\delta}$specimens with substitution concentration (x=y=0, 0.2, 0.4)

Table4- 2:magnitudes of a,b,c,c/a ratio,volume,mass density, v2212,v2223 and crystal size of
$Bi_{2-x}Pb_xSr_2Ca_2\ Cu_{3-y}Ni_yO_{2n+4+\delta}$ specimens.

specimen	a($A°$)	b($A°$)	C($A°$)	c/a	Volume ($A°$)^3	ρ_m (g/cm^3)	$V_{ph-2223}$	$V_{ph-2212}$	Crys. size (nm)
$Bi_2Sr_2Ca_2\ Cu_3O_{10+\delta}$	5.439	5.4621	36.992	6.8	1098.97	1.548	77.1%	22.6%	40.9009
$Bi_{1.8}Pb_{0.2}Sr_2Ca_2Cu_{2.8}Ni_{0.2}O_{10+\delta}$	5.395	5.389	37.735	6.99	1097.09	1.557	79%	20.3%	39.626
$Bi_{1.6}Pb_{0.4}Sr_2Ca_2\ Cu_{2.6}Ni_{0.4}O_{10+\delta}$	5.391	5.383	37.782	7.01	1096.42	1.556	80%	19.6%	39.034
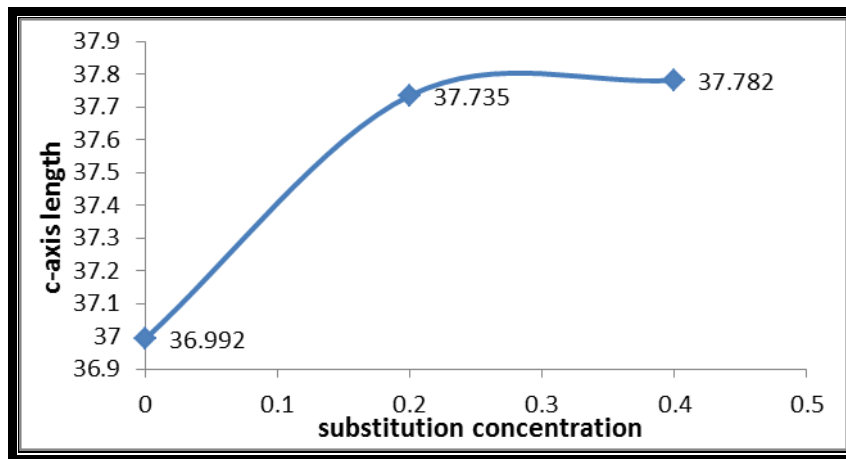
Figure4- 5: relation between c-axis length and substitution concentration $Bi_{2-x}Pb_xSr_2Ca_2\ Cu_{3-y}Ni_yO_{2n+4+\delta}$ of specimens.

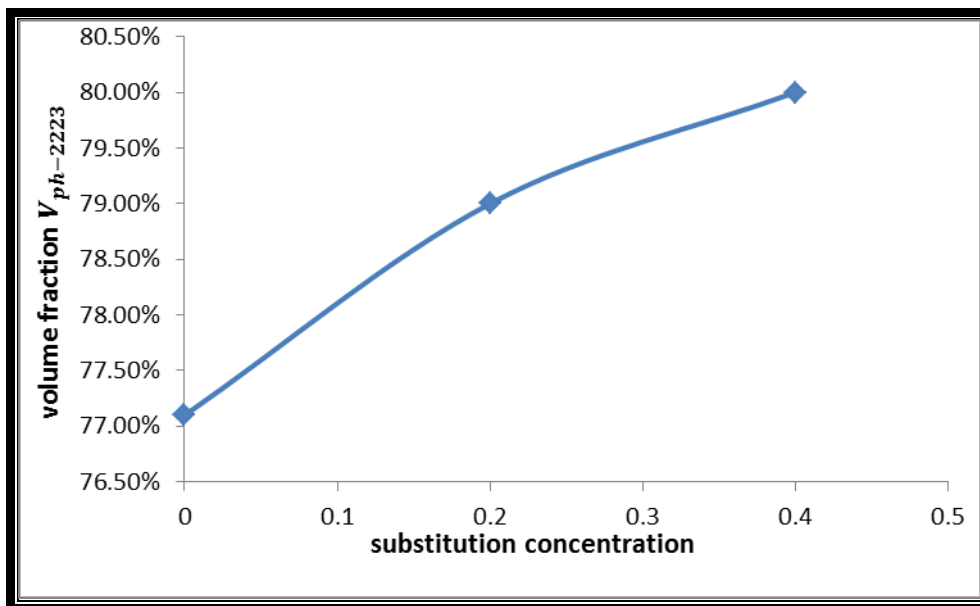**Figure4- 6:relation between volume fraction $V_{ph-2223}$ and substitution concentration of $Bi_{2-x}Pb_xSr_2Ca\ Cu_{2-y}Ni_yO_{2n+4+\delta}$ specimens.**

4.2.2 Fast neutron influence on structure of fabricated specimens:

The influence of irradiation by fast neutrons using $^{241}Am/Be$ source with energy of 5 Mev and flux of 10^5 neutron/Cm^2.sec, for two weak ($1.296*10^{11}$neutron/cm^2) on structure of $Bi_{2-x}Pb_xSr_2Ca_{n-1}\,Cu_{n-y}Ni_yO_{2n+4+\delta}$ (n=2 and 3, (x=y=0, 0.2 and 0.4) were investigated by x-ray diffraction. The results of XRD after irradiation demonstrated that there is no phase transformations take place for all specimens' structures, where the irradiated specimens found that it had an orthorhombic structure like the non-irradiated specimens. All samples structures undergo a change in the lattice parameters after irradiation lattice distortion produced by irradiation [72].   The changes happened in structure due to fast neutron irradiation it will be written in the form of points:

1-XRD pattern of irradiated $Bi_{2-x}Pb_xSr_2Ca_n\,Cu_{2-y}Ni_yO_{8+\delta}$ specimens was illustrated in Figure (4-7). There is very small shift in the peaks position and increase in peaks intensities of $Bi_2Sr_2Ca\,Cu_2O_{8+\delta}$ so high-$T_c$phase volume fraction$V_{ph-2223}$ was increased after irradiation as listed in Table (4-3). While $Bi_{1.8}Pb_{0.2}Sr_2Ca\,Cu_{1.8}Ni_{0.2}O_{8+\delta}$ and $Bi_{1.6}Pb_{0.4}Sr_2Ca\,Cu_{1.6}Ni_{0.4}O_{8+\delta}$ specimens exhibit decrease in peaks intensities. The calculated lattice parameters were changed after irradiation as listed in Table (4-3), where a-axis and b-axis were change and C-axis was increased, this increase attributed to movement of oxygen atoms to crystal surface causing increasing in Cu-O bond length [72, 83]. The volume of unite cell change due to lattice parameters change, thus the density affected by fast neutron irradiation as listed in Table(4-3)

2-XRD pattern of $Bi_{2-x}Pb_xSr_2Ca_2\,Cu_{3-y}Ni_yO_{10+\delta}$ is illustrated in Figure *(4-8)*. It is noted that the peaks exhibit very small shifting toward lower angles, and the intensities of peaks was decreased after exposed to fast

neutron irradiation for all specimens. Results of estimated lattice parameters before and after irradiation were involved in Table (4-3), it is found there are changes in a-axis and b-axis for all specimens. And c-axis of $Bi_2Sr_2Ca_2Cu_3O_{10+\delta}$ increases due to movement of oxygen atoms to crystal surface causing increasing in Cu-O bond length[72,83].

While c-axis of $Bi_{1.8}Pb_{0.2}Sr_2Ca_2Cu_{2.8}Ni_{0.2}O_{10+\delta}$ and $Bi_{1.6}Pb_{0.4}Sr_2Ca_2Cu_{2.6}Ni_{0.4}O_{10+\delta}$ specimens exhibit decrease in theirs length, these decreases attributed to ability of neutron to penetrate the surface of layers causing oxygen atoms to displaced [72], thus the volume of unit cell and density affected, and theirs values were listed in Table (4-3). The volume fraction V_{ph} of high temperature phase was decreased as listed in Table (4-3). Crystallite size also affected after fast neutron irradiation as listed in Table (4-3).

Table4- 3:magnitudes of lattice parameters, c/a ratio,volume,mass densityn v2212,v2223 and crystal size for all specimens after irradiated by fast neutron.

Specimen(n)	$a(A°)$	$b(A°)$	$C(A°)$	c/a	Volume	ρ_m (g/cm^3)	V-Hpeak	Crys. size (nm)
$Bi_2Sr_2Ca Cu_2O_{8+\delta}$	5.372	5.413	30.981	5.767	900.88	1.638	78.8%	34.6
$Bi_{1.8}Pb_{0.2}Sr_2Ca Cu_{1.8}Ni_{0.2}O_{8+\delta}$	5.415	5.391	31.12	5.746	908.46	1.622	77.6%	32.439
$Bi_{1.6}Pb_{0.4}Sr_2Ca Cu_{1.6}Ni_{0.4}O_{8+\delta}$	5.43	5.38	31.31	5.766	914.67	1.607	78.5%	33.056
$Bi_2Sr_2Ca_2 Cu_3O_{10+\delta}$	5.437	5.432	37.154	6.833	1097.29	1.544	75.2%	39.719
$Bi_{1.8}Pb_{0.2}Sr_2Ca_2Cu_{2.8}Ni_{0.2}O_{10+\delta}$	5.437	5.441	37.218	6.84	1101	1.54867	77.3%	41.052
$Bi_{1.6}Pb_{0.4}Sr_2Ca_2 Cu_{2.6}Ni_{0.4}O_{10+\delta}$	5.412	5.4351	37.322	6.89	1097.8	1.55195	77.5%	39.838
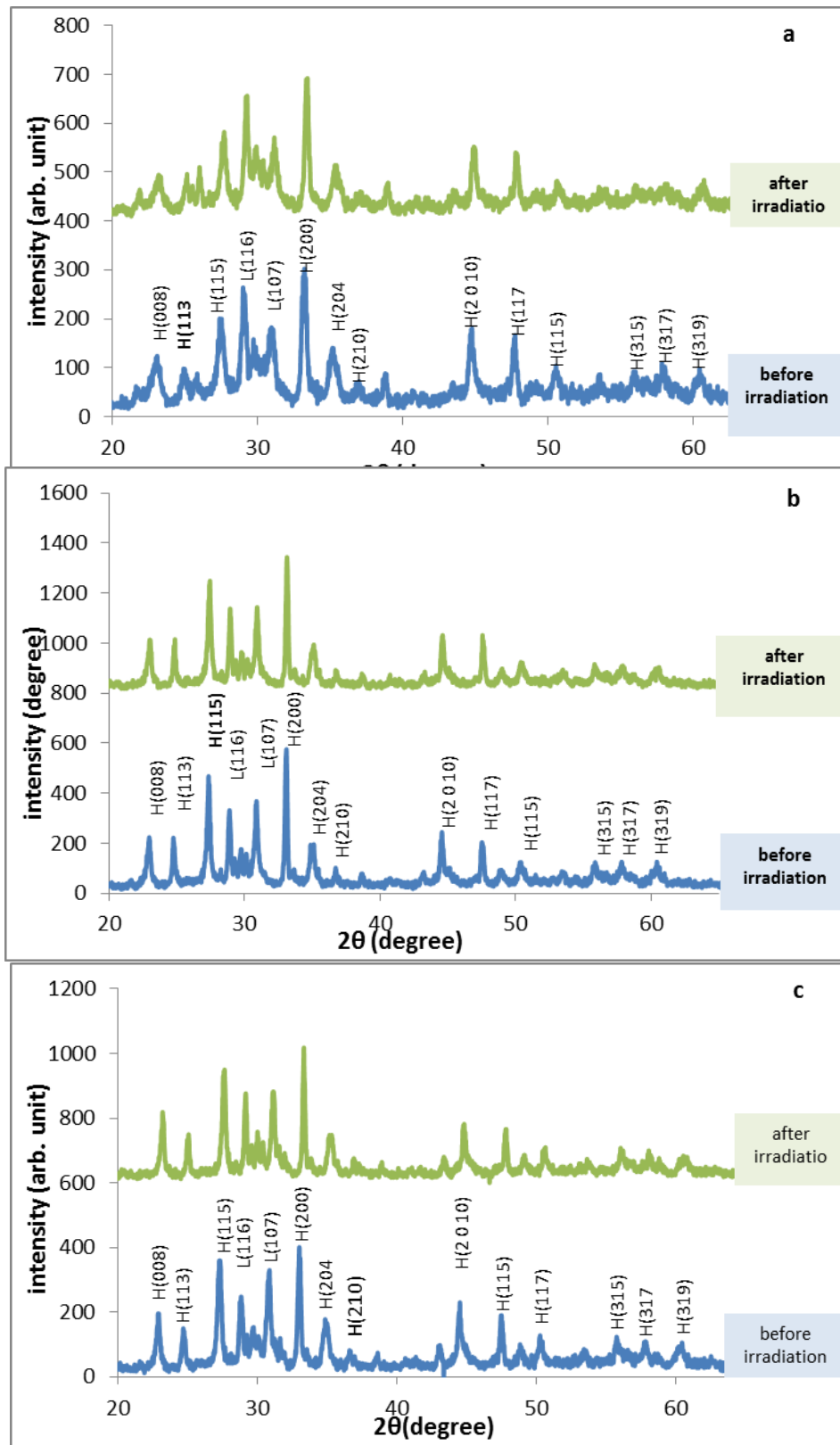
Figure4- 7:XRD patterns of $Bi_{2-x}Pb_xSr_2Ca\ Cu_{2-y}Ni_yO_{8+\delta}$ **specimens after exposed to neutrons irradiation (a:x=y=0),(b:x=y=0.2),(c:x=y=0.4)**.

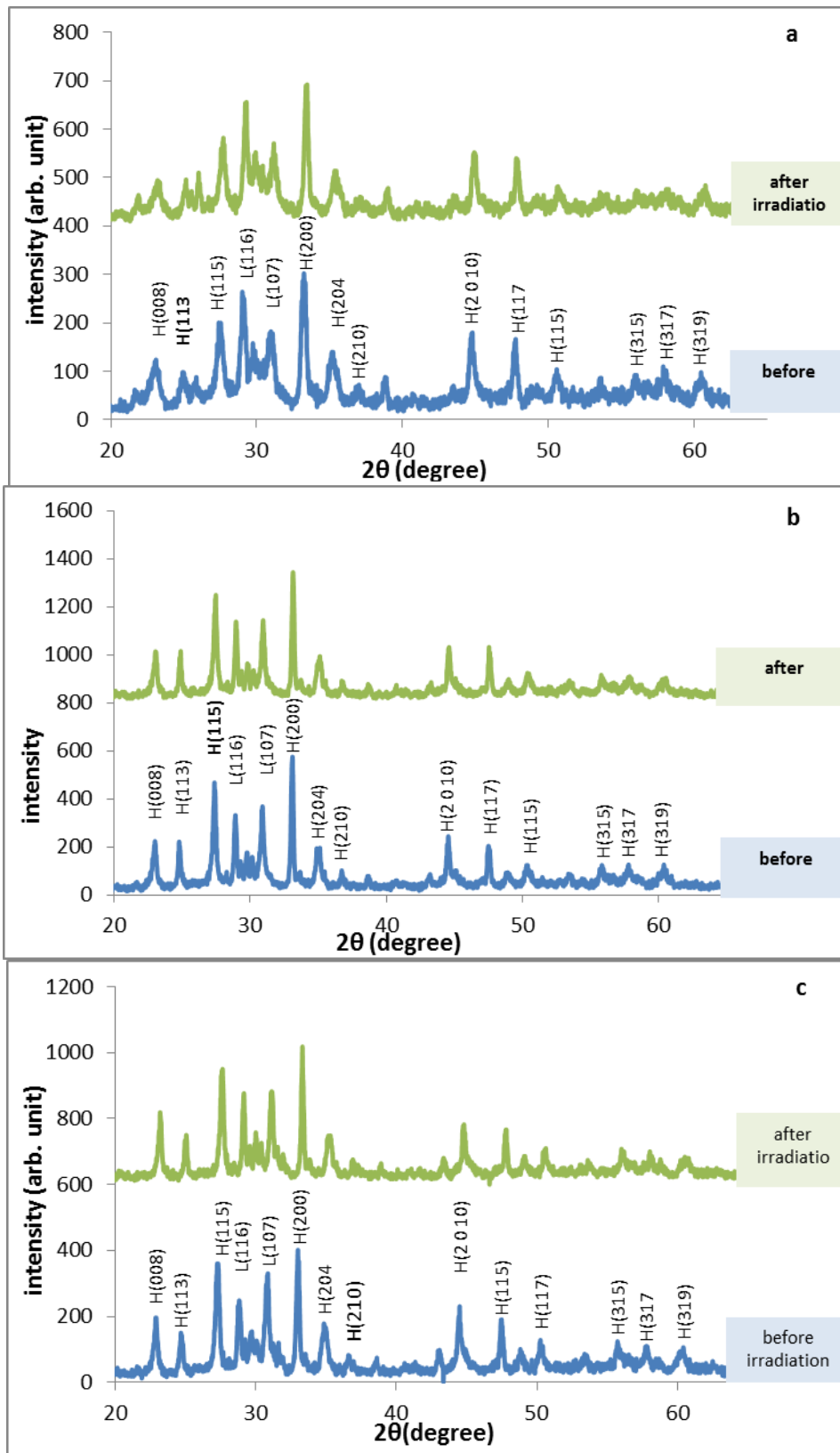**Figure4- 8:XRD patterns of** $Bi_{2-x}Pb_xSr_2Ca_2Cu_{3-y}Ni_yO_{10+\delta}$ **specimens after exposed to fast neutron irradiation (a:x=y=0),(b:x=y=0.2),(c:x=y=0.4).**

49

4.2.3 Laser influence on structure of fabricated specimens:

The influence of diode – laser irradiation on the structure properties of $Bi_{2-x}Pb_xSr_2Ca_n Cu_{n-y}Ni_yO_{8+\delta}$ compound with substitution concentration (x=y=0, 0.2 and 0.4) was investigated utilizing XRD analysis. Results of XRD explained that there are no phase's transformations take place after laser irradiation, where the irradiated specimens have orthorhombic crystal structure too, but there are changes in peaks intensities and estimated lattice parameters were noted. The changes happened in structure due laser irradiation, it will be written in the form of points.

1-XRD pattern of $Bi_{2-x}Pb_xSr_2Ca Cu_{2-y}Ni_yO_{8+\delta}$ specimens with substitution concentration (x=y=0, 0.2 and 0.4) was illustrated in Figure (4-9).It is noted that $Bi_2Sr_2Ca Cu_2O_{8+\delta}$ undoped specimen (x=y=0) exhibits a small shift in peaks positions toward lower angles and clear increase in peaks intensities after irradiation and increase volume fraction of highT_C phase $V_{ph-2212}$, this indicates the improvement of crystalline structure [59]. The calculated lattice parameters were listed in Table (4-4), a-axis and b-axis exhibit change due to irradiation. C-axis length shows increase after irradiation.

For $Bi_{1.8}Pb_{0.2}Sr_2Ca Cu_{1.8}Ni_{0.2}O_{8+\delta}$ specimen (x=y=0.2) XRD pattern exhibits small shift in peaks positions toward higher angles and peaks intensities increase by magnitude small than that of (x=y=0). The volume fraction $V_{ph-2212}$ shows increase in its value, this is also evidence of improved crystal structure [59]. a-axis and b-axis changed in addition to increase in c-axis length as listed in Table(4-4). The crustal structure was improved may attributed to thermal treatment caused by absorption of laser ray.

For $Bi_{1.6}Pb_{0.6}Sr_2Ca\ Cu_{1.6}Ni_{0.4}O_{8+\delta}$ specimen (x=y=0.4) XRD pattern exhibits small shift in peaks positions toward higher angles and a decrease in peaks intensities. Unlike other specimens, the volume fraction $V_{ph-2212}$ shows decrease in its value, indicating the irregularity in crystal structure caused by irradiation. A-axis and b-axis changed in addition to decrease in c-axis length as listed in Table (4-4). The volume of unit cell values changed as lattice parameters change, thus the density of all specimens also affected by laser irradiation

2-XRD pattern of $Bi_{2-x}Pb_xSr_2Ca_2\ Cu_{3-y}Ni_yO_{10+\delta}$ specimens with substitution concentrations (x=y=0, 0.2 and 0.4) were shown in Figure (4-10). It is observed that $Bi_2Sr_2Ca_2\ Cu_3O_{10+\delta}$ undoped specimen (x=y=0) exhibits a small shift in peaks positions toward lower angles and increase in peaks intensities after irradiation and increase volume fraction of highT_C phase $V_{ph-2223}$, this indicates the enhancement of crystalline structure. The calculated lattice parameters were listed in Table (4-4), a-axis and b-axis change after irradiation. C-axis length shows increase after irradiation.

For $Bi_{1.8}Pb_{0.2}Sr_2Ca_2Cu_{2.8}Ni_{0.2}O_{8+\delta}$ specimen (x=y=0.2) XRD pattern exhibits small shift in peaks positions toward lower angles and peaks intensities decrease. The volume fraction $V_{ph-2223}$ shows decrease in its value because of irregularity in crystal structure produced by irradiation. A-axis and b-axis changed in addition to decrease in c-axis length as listed in Table (4-4).

For $Bi_{1.6}Pb_{0.6}Sr_2Ca_2\ Cu_{2.6}Ni_{0.4}O_{8+\delta}$ specimen (x=y=0.4) XRD pattern shows small shift in peaks positions toward lower angles and an increase in peaks intensities. The volume fraction $V_{ph-2223}$ shows increase in its value. A-axis and b-axis changed in addition to increase in

c-axis length as listed in Table (4-4). The increase in high-T_C phase attributed to the same above mentioned reasons of enhanced some of (n=2) specimens after exposed to laser ray.

Table4- 4:Magnitudes of lattice parameters,c/aratio,volume,mass density, volume fraction of high peaks,and crystal size for all specimens after exposed to laser ray.

| Specimen(n)	a($A°$)	b($A°$)	C($A°$)	c/a	Volume ($A°$)^3	ρ_m (g/cm^3)	$V_{H-peaks}$	Crys. Size (nm)
$Bi_2Sr_2Ca\ Cu_2O_{8+\delta}$	5.363	5.423	30.995	5.779	901.44	1.637	79%	34.408
$Bi_{1.8}Pb_{0.2}Sr_2Ca\ Cu_{1.8}Ni_{0.2}O_{8+\delta}$	5.373	5.418	31.161	5.799	907.12	1.625	79.7%	31.947
$Bi_{1.6}Pb_{0.4}Sr_2Ca\ Cu_{1.6}Ni_{0.4}O_{8+\delta}$	5.421	5.463	30.989	5.716	917.73	1.602	77.4%	36.644
$Bi_2Sr_2Ca_2\ Cu_3O_{10+\delta}$	5.431	5.429	37.209	6.85	1097. 1	1.562	78.9%	39.139
$Bi_{1.8}Pb_{0.2}Sr_2Ca_2Cu_{2.8}Ni_{0.2}O_{10+\delta}$	5.453	5.461	37.512	6.88	1117.063	1.522	78%	41.752
$Bi_{1.6}Pb_{0.4}Sr_2Ca_2\ Cu_{2.6}Ni_{0.4}O_{10+\delta}$	5.245	5.221	37.919	7.23	1038.379	1.644	80.1%	38.052
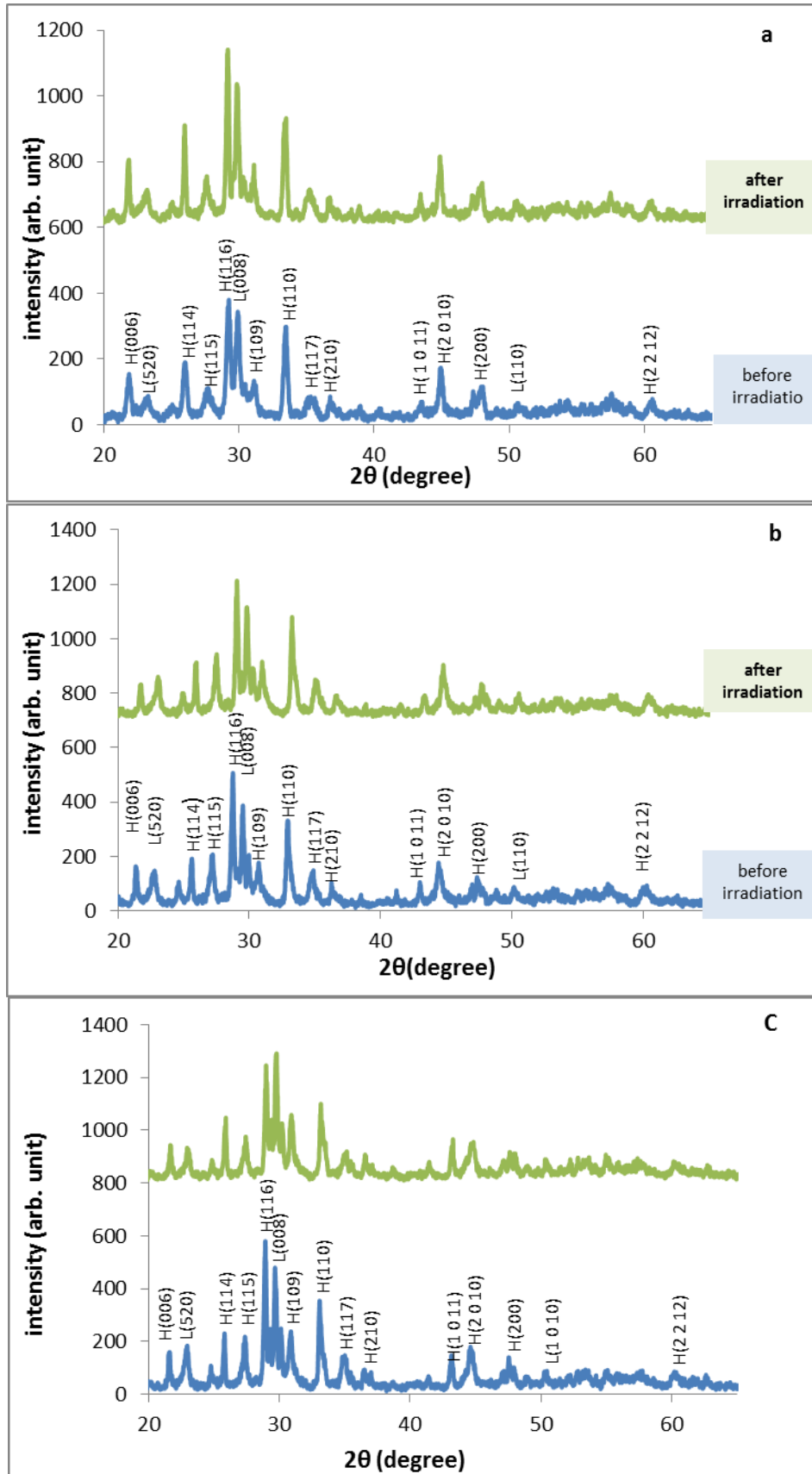
Figure4- 9:XRD pattern of $Bi_{2-x}Pb_xSr_2Ca\,Cu_{2-y}Ni_yO_{8+\delta}$specimen after exposed to laser irradiation (a:x=y=0),(b:x=y=0.2),(c:x=y=0.4).
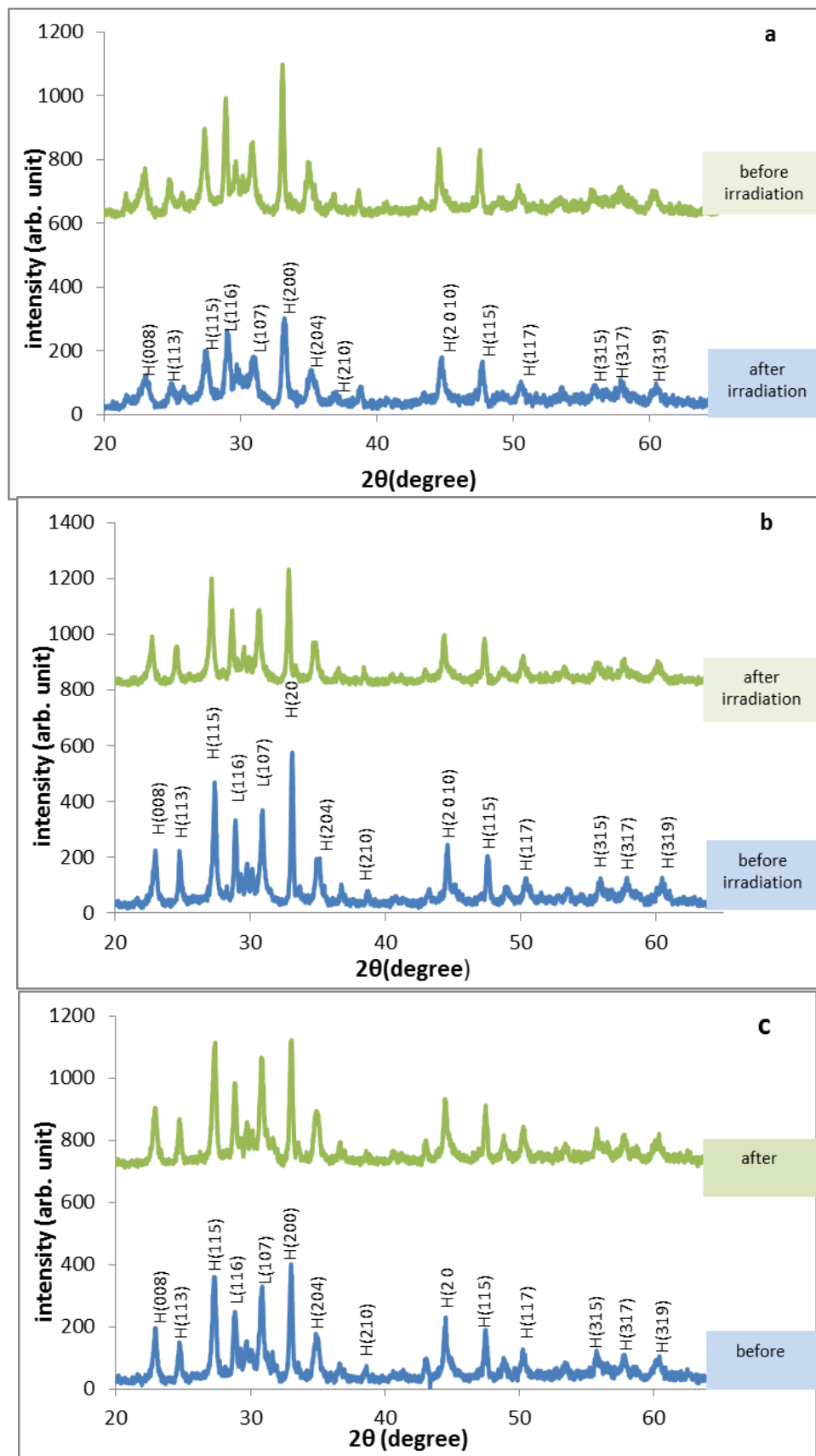
Figure4- 10:XRD pattern of specimens after exposed to laser irradiation (a:x=y=0),(b:x=y=0.2),(c:x=y=0.4).

4.2.4 **influence of Beta irradiation on structure of fabricated**

specimens :

The influence of beta particles irradiation on the structure properties of $Bi_{2-x}Pb_xSr_2Ca_n Cu_{n-y}Ni_yO_{8+\delta}$ compound with substitution concentration (x=y=0, 0.2 and 0.4) was investigated utilizing XRD analysis. Results of XRD explained that there are no phase's transformations take place after beta-particles irradiation, where the irradiated specimens have orthorhombic crystal structure too, but there are changes in peaks intensities and estimated lattice parameters were noted. The changes happened in structure due beta irradiation. It will be written in the form of points.

1-XRD pattern of $Bi_{2-x}Pb_xSr_2Ca Cu_{2-y}Ni_yO_{8+\delta}$ specimens with substitution concentration (x=y=0, 0.2 and 0.4) was illustrated in Figure (4-11).It is noted that $Bi_2Sr_2Ca Cu_2O_{8+\delta}$ undoped specimen (x=y=0) exhibits a small shift in peaks positions toward lower angles and increase in peaks intensities. Volume fraction of highT_C phase $V_{ph-2212}$ has increased. The lattice parameters was calculated after expose to beta-particles and listed in Table (4-5), a-axis and b-axis exhibit change due to irradiation. C-axis length shows increase after irradiation.

For $Bi_{1.8}Pb_{0.2}Sr_2Ca Cu_{1.8}Ni_{0.2}O_{8+\delta}$ specimen (x=y=0.2) XRD pattern exhibits small shift in peaks positions toward higher angles and peaks intensities increase by magnitude small than that of (x=y=0). The volume fraction $V_{ph-2212}$ shows small increase in its value, this is also evidence of improved crystal structure. a-axis and b-axis change in addition to increase in c-axis length as listed in table(4-5).

For $Bi_{1.6}Pb_{0.6}Sr_2Ca\,Cu_{1.6}Ni_{0.4}O_{8+\delta}$ specimen (x=y=0.4) XRD pattern exhibits small shift in peaks positions toward higher angles and a decrease in H-peaks (2212) intensities and decrease in L-peaks(2201) intensities . Unlike other specimens, the volume fraction $V_{ph-2212}$ shows decrease in its value, indicating the irregularity in crystal structure caused by irradiation. A-axis and b-axis change in addition to decrease in c-axis length as listed in Table (4-11)

2-XRD pattern of $Bi_{2-x}Pb_xSr_2Ca_2\,Cu_{3-y}Ni_yO_{10+\delta}$ specimens with substitution concentrations (x=y=0, 0.2 and 0.4) were shown in Figure (4-12). It is observed that $Bi_2Sr_2Ca_2\,Cu_3O_{10+\delta}$ undoped specimen (x=y=0) exhibits a small shift in peaks positions toward lower angles and increase in peaks intensities after irradiation and increase volume fraction of highT_C phase $V_{ph-2223}$, this indicates the enhancement of crystalline structure. The calculated lattice parameters were listed in Table (4-5), a-axis and b-axis change after irradiation. C-axis length shows increase after irradiation.

For $Bi_{1.8}Pb_{0.2}Sr_2Ca_2Cu_{2.8}Ni_{0.2}O_{8+\delta}$ specimen (x=y=0.2) XRD pattern exhibits small shift in peaks positions toward lower angles and peaks intensities increase. The volume fraction $V_{ph-2223}$ shows increase in its value. A-axis and b-axis change in addition to decrease in c-axis length as listed in Table (4-5).

For $Bi_{1.6}Pb_{0.6}Sr_2Ca_2\,Cu_{2.6}Ni_{0.4}O_{8+\delta}$ specimen (x=y=0.4) XRD pattern shows small shift in peaks positions toward higher angles and an increase in peaks intensities. The volume fraction $V_{ph-2223}$ shows increase in its value. A-axis and b-axis change in addition to increase in c-axis length as listed in Table(4-5).

changes of a-axis, b-axis and c-axis length of beta irradiated specimens because beta particles interact with substance by ionization, excitation of electron orbital or bremsstrahlung mechanisms, thus the interaction may change of electrons in to anti bonding orbital. The change in electrons in to anti bonding orbital produce change in Cu-O bond length (increase or decrease) [5].

Table4- 5:magnitudes of lattice parameters,c/a ratio,volume,volume fraction of high peaks,mass density and crystal size for all specimens after exposed to beta irradiation.

| Specimen(n)	$a(A^°)$	$b(A^°)$	$C(A^°)$	c/a	Volume $(A^°)^3$	$V_{H-peaks}$	ρ_m $_{(g/cm^3}$	Crys. Size (nm)
$Bi_2Sr_2Ca\ Cu_2O_{8+\delta}$	5.372	5.432	31.051	5.78	906.09	79.76%	1.63	31.834
$Bi_{1.8}Pb_{0.2}Sr_2Ca\ Cu_{1.8}Ni_{0.2}O_{8+\delta}$	5.391	5.409	31.121	5.77	907.48	79.4%	1.62	31.997
$Bi_{1.6}Pb_{0.4}Sr_2Ca\ Cu_{1.6}Ni_{0.4}O_{8+\delta}$	5.432	5.469	30.897	5.68	917.87	73.12%	1.60	36.211
$Bi_2Sr_2Ca_2\ Cu_3O_{10+\delta}$	5.43	5.409	37.112	6.83	1090.01	77.5%	1.57	37.074
$Bi_{1.8}Pb_{0.2}Sr_2Ca_2\ Cu_{2.8}Ni_{0.2}O_{10+\delta}$	5.436	5.426	37.439	6.88	1104.29	80%	1.55	41.784
$Bi_{1.6}Pb_{0.4}Sr_2Ca_2\ Cu_{2.6}Ni_{0.4}O_{10+\delta}$	5.383	5.372	37.945	7.04	1097.27	81%	1.55	39.712
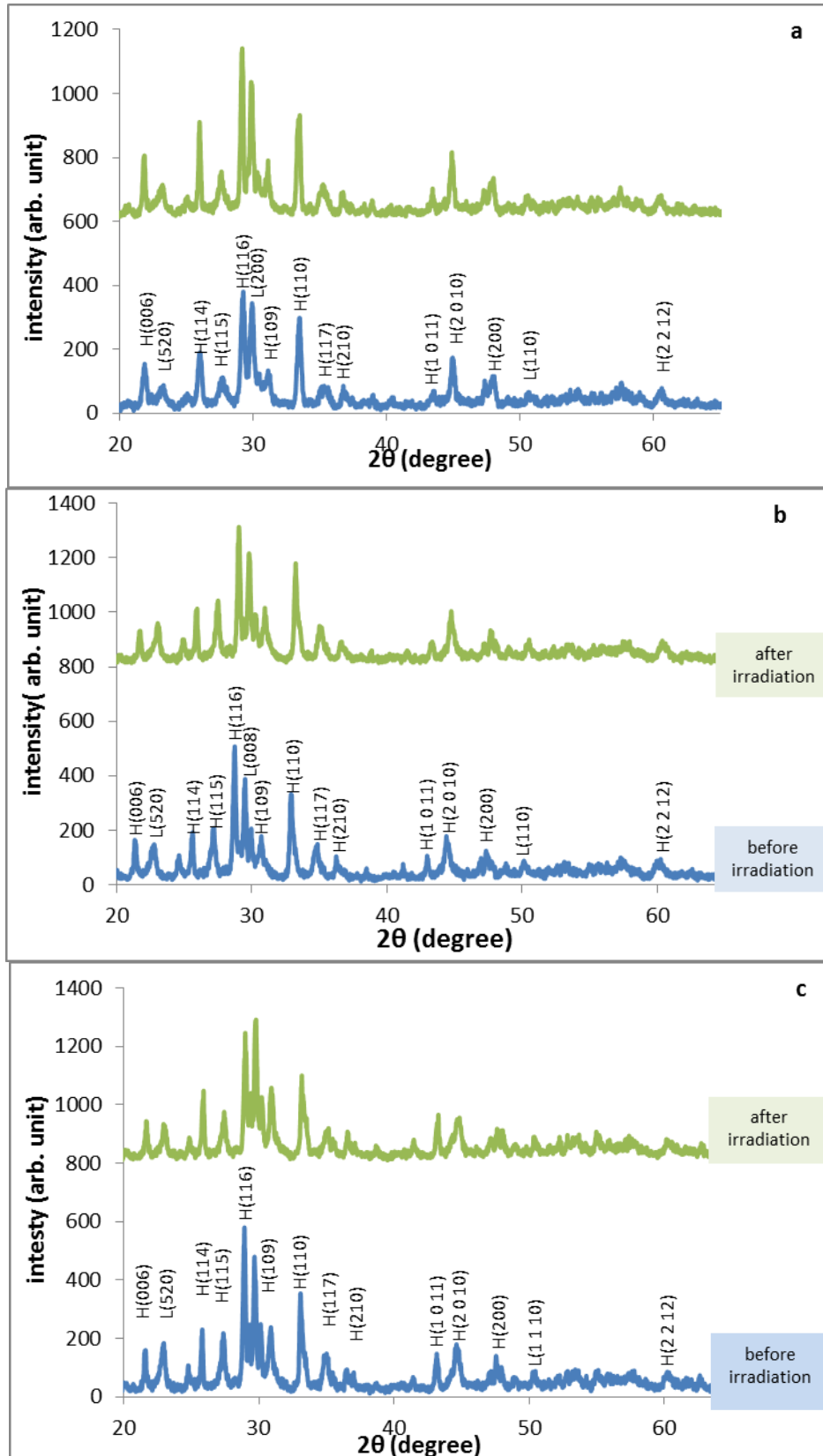
Figure4- 11:XRD diffraction pattern of $Bi_{2-x}Pb_xSr_2Ca\ Cu_{2-y}Ni_yO_{8+\delta}$specimen after exposed to beta irradiation (a:x=y=0)(b:x=y=0.2)(c:x=y=0.4).

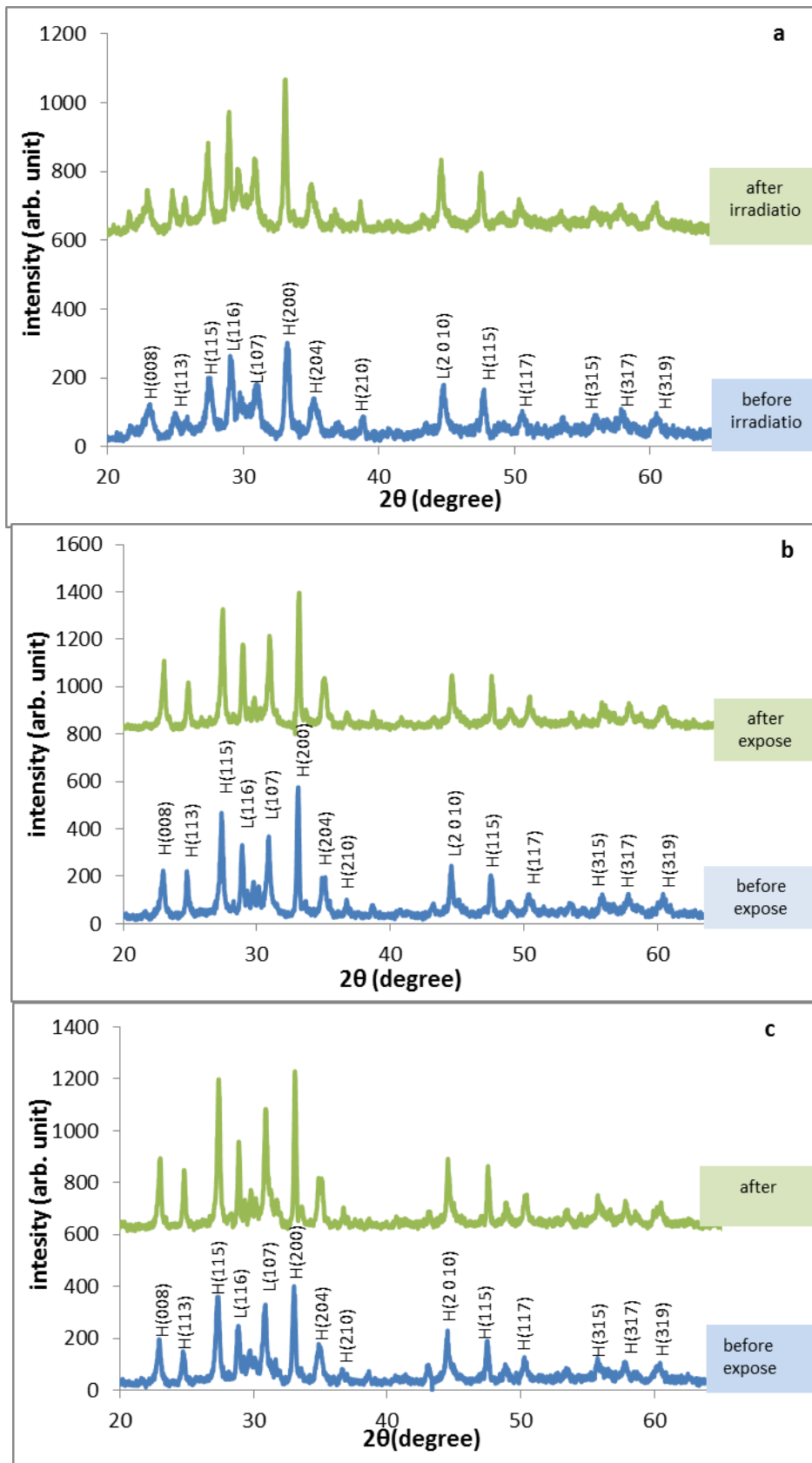**Figure4- 12:XRD pattern of $Bi_{2-x}Pb_xSr_2Ca_2Cu_{3-y}Ni_yO_{8+\delta}$specimens after exposed to laser irradiation (a:x=y=0),(x=y=0.2),(c:x=y=0.4).**

4.3 **Iodometric Titration:**

Oxygen content was calculated in fabricated samples before and after irradiation by different categories of irradiation by Iodometric titration method. The results showed that there is a close correlation between the critical temperature and the oxygen content as shown in the tables of results. This correlation was observed by the results of critical temperature and oxygen content, which may attributed to that the increase of oxygen atoms in the Cu-O_2 layers leads to the creation of holes in the Cu-O_2 sheet resulting in a reduction of the length of the Cu-O_2 bond, so it can be observed that the increase in oxygen content (δ) can generate increase in critical temperature, and there is optimum magnitude of oxygen content (δ) at which the critical temperature achieve a highest magnitude. From the results of Table (4-6) it is possible to observe that there is an increase in the oxygen content associated with the increase of the substitution concentration (x, y) for each (n) value, this increase is due to the fact that the replacement of (Bi^{+3}) by lead ion (Pb^{+2}) effects on charge balance oxygen content [53,84] and the copper(Cu^{+2}) replacement by nickel (Ni^{+3})already act on alter oxygen content values by carry more charge to Cu-O_2layers causing oxidation some of Cu atoms to(Cu^{+3}). Presence of Cu^{+2}/ Cu^{+3} hybrid situation produce improvement of superconductivity [35,85].

The results of iodometric test after specimens exposed to fast neutron irradiation explained that there are decreases in oxygen content of $(Bi_{1.8}Pb_{0.2}Sr_2Ca\ Cu_{1.8}Ni_{0.2}O_{8+\delta})$, $(Bi_{1.6}Pb_{0.4}Sr_2Ca\ Cu_{1.6}Ni_{0.4}O_{8+\delta})$, $(Bi_2Sr_2Ca_2\ Cu_3\ O_{10+\delta})$ $(Bi_{1.8}Pb_{0.2}Sr_2Ca_2\ Cu_{2.8}Ni_{0.2}O_{10+\delta})$ and $(Bi_{1.6}Pb_{0.4}Sr_2Ca_2\ Cu_{2.6}Ni_{0.4}O_{10+\delta})$, as listed in Table (4-6), these decreases attributed to the fact that the neutron is able to penetrate the surface of layers and thus the oxygen atoms displaced [72]. It can be observed from Table (4-6), that $Bi_2Sr_2Ca\ Cu_2O_{8+\delta}$ Exhibit increase in its oxygen content value after fast neutron irradiation due to rising of temperature as a result of thermal impact caused by irradiation [72].

The results of iodometric test after laser irradiation explained that oxygen content of $Bi_2Sr_2Ca\ Cu_2O_{8+\delta}$, $Bi_{1.8}Pb_{0.2}Sr_2Ca\ Cu_{1.8}Ni_{0.2}O_{8+\delta}$,

$Bi_2Sr_2Ca_2\ Cu_3O_{10+\delta}$, and $Bi_{1.6}Pb_{0.4}Sr_2Ca_2\ Cu_{2.6}Ni_{0.4}O_{10+\delta}$ specimens exhibited increases, these increases may attribute to specimens temperature increase during laser irradiation causes specimens thermal treatment, and these increases caused increase high T_c phase volume fraction as showed in XRD patterns. While $Bi_{1.6}Pb_{0.4}Sr_2Ca\ Cu_{1.6}Ni_{0.4}O_{8+\delta}$ and $Bi_{1.8}Pb_{0.2}Sr_2Ca_2\ Cu_{2.8}Ni_{0.2}O_{10+\delta}$ specimens exhibit decrease in theirs oxygen content values after laser irradiation because that laser ray may be cause Break some of the bonds in the cu-o plane Perovskite structure, which directly affects the content of oxygen.

Results of iodometric test after specimens exposed to beta irradiation explained that $(Bi_2Sr_2Ca\ Cu_2O_{8+\delta})$, $(Bi_{1.8}Pb_{0.2}Sr_2Ca\ Cu_{1.8}Ni_{0.2}O_{8+\delta})$, $(Bi_{1.8}Pb_{0.2}Sr_2Ca_2\ Cu_{2.8}Ni_{0.2}O_{10+\delta})$ $(Bi_{1.6}Pb_{0.4}Sr_2Ca_2\ Cu_{2.6}Ni_{0.4}O_{10+\delta})$ and $(Bi_2Sr_2Ca_2\ Cu_3O_{10+\delta})$ specimens exhibited increasing in theirs oxygen contents values after exposed to beta irradiation, these increases may attributed to ability of beta particles to interacts with substance by

ionization, electron orbital excitation or bremsstrahlung interaction mechanism [80], these interaction caused improvement of crystal structure or cause electrons structure change, so oxygen contents were enhanced as listed in Table (4-6), while these interactions play negative role with $Bi_{1.6}Pb_{0.4}Sr_2Ca\ Cu_{1.6}Ni_{0.4}O_{8+\delta}$, where the oxygen content decreased after beta irradiation of this specimens.

Table4- 6:Magnitudes of oxygen content for all specimens before and after exposed to fast neutrons irradiation, laser irradiation and beta irradiation.

specimen	Oxygen content(δ) before irradiation	Oxygen content (δ) after fast neutron irradiation	Oxygen content (δ) after laser irradiation	Oxygen content (δ) after beta irradiation
$Bi_2Sr_2Ca\ Cu_2O_{8+\delta}$	0.04185	0.053491	0.05872	0.1095
$Bi_{1.8}Pb_{0.2}Sr_2Ca\ Cu_{1.8}Ni_{0.2}O_{8+\delta}$	0.04924	0.03739	0.06418	0.06719
$Bi_{1.6}Pb_{0.4}Sr_2Ca\ Cu_{1.6}Ni_{0.4}O_{8+\delta}$	0.06092	0.039817	0.04824	0.0328
$Bi_2Sr_2Ca_2\ Cu_3O_{10+\delta}$	0.39194	0.19835	0.50165	0.4387
$Bi_{1.8}Pb_{0.2}Sr_2Ca_2\ Cu_{2.8}Ni_{0.2}O_{10+\delta}$	0.4192	0.2693	0.118	0.5601
$Bi_{1.6}Pb_{0.4}Sr_2Ca_2\ Cu_{2.6}Ni_{0.4}O_{10+\delta}$	0.4237	0.3016	0.4619	0.5295

4.4 Results of electrical properties of prepared specimens:

4.4.1 Influence of Pb and Ni substitution on electric properties of (BSCCO):

Four probes technique was used to estimate the critical temperature T_c of prepared specimens to determine the substitution concentration which has higher T_c and also to investigate the influence of different categories of irradiation on critical temperature of prepared specimens. Critical temperature T_c Measurement results of

$Bi_{2-x}Pb_xSr_2Ca\ Cu_{2-y}Ni_yO_{8+\delta}$ (2212) and $Bi_{2-x}Pb_xSr_2Ca_2\ Cu_{3-y}Ni_yO_{10+\delta}$ (2223) specimens with substitution (x=y=0, 0.2 and 0.4) explained that there are increases in T_c with increase of substitution concentration for both systems (2212 and 2223). These increases take place because the partial substitution of Bi by Pb atoms allows to prepares of high-T_c phase with the variation of Cu valence from 2^+to3^+, where the quantity of Cu^{+3}ions play important role in determine of T_C. Moreover, the partial substitution increases the tolerance factor and causes the enhancement of the chemical stability so that the superconducting properties are affected [53] [69] [86]. Figure (4-13) (4-14) illustrate absolute temperature vs. electrical resistivity of (2212) and (2223) respectively.

Table4- 6: Magnitudes of critical temperatures of all specimens before irradiated.

specimen	$T_{c(offset)}$	$T_{c(onset)}$	$T_{c(mid)}$
$Bi_2Sr_2Ca\ Cu_2O_{8+\delta}$	85	97	92
$Bi_{1.8}Pb_{0.2}Sr_2Ca\ Cu_{1.8}Ni_{0.2}O_{8+\delta}$	88	108	98
$Bi_{1.6}Pb_{0.4}Sr_2Ca\ Cu_{1.6}Ni_{0.4}O_{8+\delta}$	93	109	101
$Bi_2Sr_2Ca_2\ Cu_3O_{10+\delta}$	111	117	114
$Bi_{1.8}Pb_{0.2}Sr_2Ca_2\ Cu_{2.8}Ni_{0.2}O_{10+\delta}$	115	117	116
$Bi_{1.6}Pb_{0.4}Sr_2Ca_2\ Cu_{2.6}Ni_{0.4}O_{10+\delta}$	117	140	128
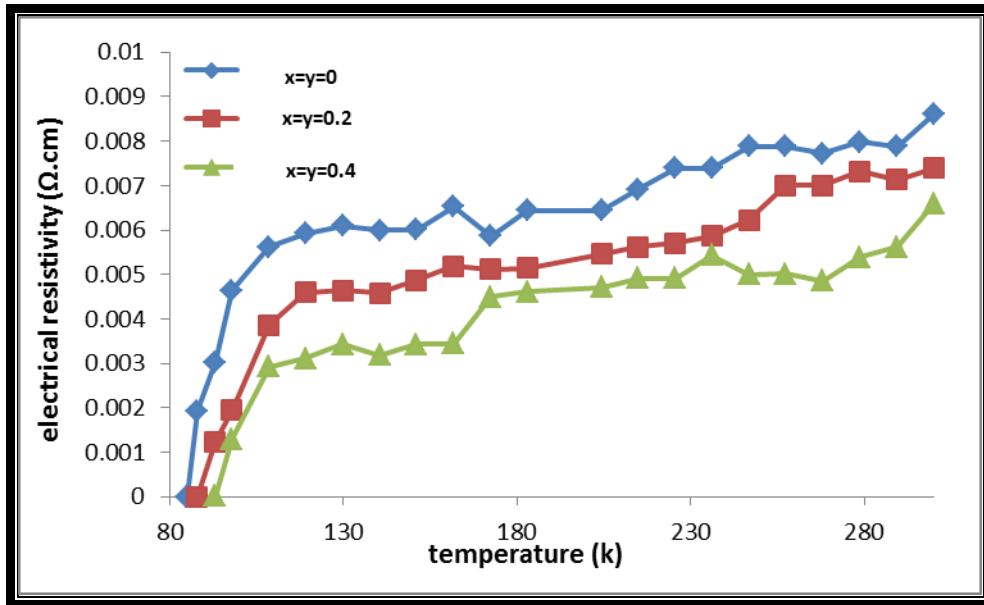
Figure4- 13:Absolute temperatur vs. electrical resistivity of
$Bi_{2-x}Pb_xSr_2Ca\,Cu_{2-y}Ni_yO_{8+\delta}$**specimens with substitution concentration**
of (x=y=0,0.2 and 0.4).
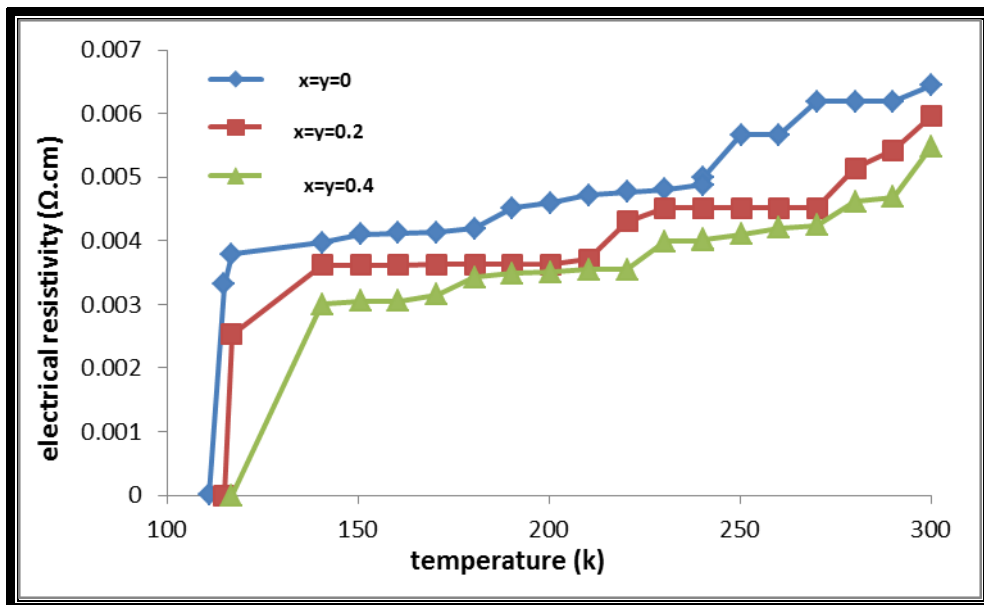
Figure4- 14: Absolute temperature vs. electrical resistivity of
$Bi_{2-x}Pb_xSr_2Ca_2Cu_{3-y}Ni_yO_{10+\delta}$**specimens with substitution**
concentration(x=y=0,0.2 and 0.4).

4.4.2 <u>Results of fast neutron effect on critical temperature of</u>

<u>fabricated   specimens:</u>

Four probes test results explained that $Bi_{2-x}Pb_xSr_2Ca\ Cu_{n-y}Ni_yO_{8+\delta}$ with (n=2 and 3) specimens with substitution concentration (x=y=0, 0.2 and 0.4) exhibited changes due expose to fast neutrons irradiation, where it is noted that $Bi_2Sr_2Ca\ Cu_2O_{8+\delta}$ undoped specimen (x=y=0) exhibits increase in its critical temperature by approximately 7K after expose to fast neutron radiation. Thermal impact happened during irradiation, the increase of temperature may improve the superconducting phase and the T_c increased as a result of this improvement [72].

For $Bi_{1.8}Pb_{0.2}Sr_2Ca\ Cu_{1.8}Ni_{0.2}O_{8+\delta}$, $Bi_{1.6}Pb_{0.6}Sr_2Ca\ Cu_{1.6}Ni_{0.4}O_{8+\delta}$, $Bi_2Sr_2Ca_2\ Cu_3O_{10+\delta}$, $Bi_{1.8}Pb_{0.2}Sr_2Ca_2\ Cu_{2.8}Ni_{0.2}O_{10+\delta}$ and $Bi_{1.6}Pb_{0.4}Sr_2Ca_2\ Cu_{2.6}Ni_{0.4}O_{10+\delta}$ specimens the results explained there are decreases in their T_c after exposed to fast neutrons irradiation by approximately 7K ,9K,6.5K,6.5K and 7K respectively as illustrated in Figures(4-15)(4-16) and listed in Table (4-8). These decreases attributed to oxygen content magnitude changing which located in small point defects (oxygen vacancies) and irradiation may damage bond in Cu-O plane, another reasons are shifting of some atoms in the crystalline lattice as a result of consecutive beatings due to cluster defects and the concentration of overlapping defects, and the damage of weak link between grains due to irradiation [58,72, 87].

Table4- 7:Magnitudes of critical temperature of all specimens after fast neutron irradiation.

Specimen	$T_{c(offset)}$	$T_{c(onset)}$	$T_{c(mid)}$
$Bi_2Sr_2Ca\ Cu_2O_{8+\delta}$	92	108	100
$Bi_{1.8}Pb_{0.2}Sr_2Ca\ Cu_{1.8}Ni_{0.2}O_{8+\delta}$	83	108	98
$Bi_{1.6}Pb_{0.4}Sr_2Ca\ Cu_{1.6}Ni_{0.4}O_{8+\delta}$	85	93	89
$Bi_2Sr_2Ca_2\ Cu_3O_{10+\delta}$	104.5	119	114
$Bi_{1.8}Pb_{0.2}Sr_2Ca_2\ Cu_{2.8}Ni_{0.2}O_{10+\delta}$	108.5	117	112.5
$Bi_{1.6}Pb_{0.4}Sr_2Ca_2\ Cu_{2.6}Ni_{0.4}O_{10+\delta}$	110	117	113.5

Figure4- 15: Absolute temperature vs. electrical resistivity of
$Bi_{2-x}Pb_xSr_2Ca\ Cu_{2-y}Ni_yO_{8+\delta}$**specimens after exposed to fast neutron irradiation with substitution concentration (a:x=y=0)(b:x=y=0.2) and x=y=0.4).**
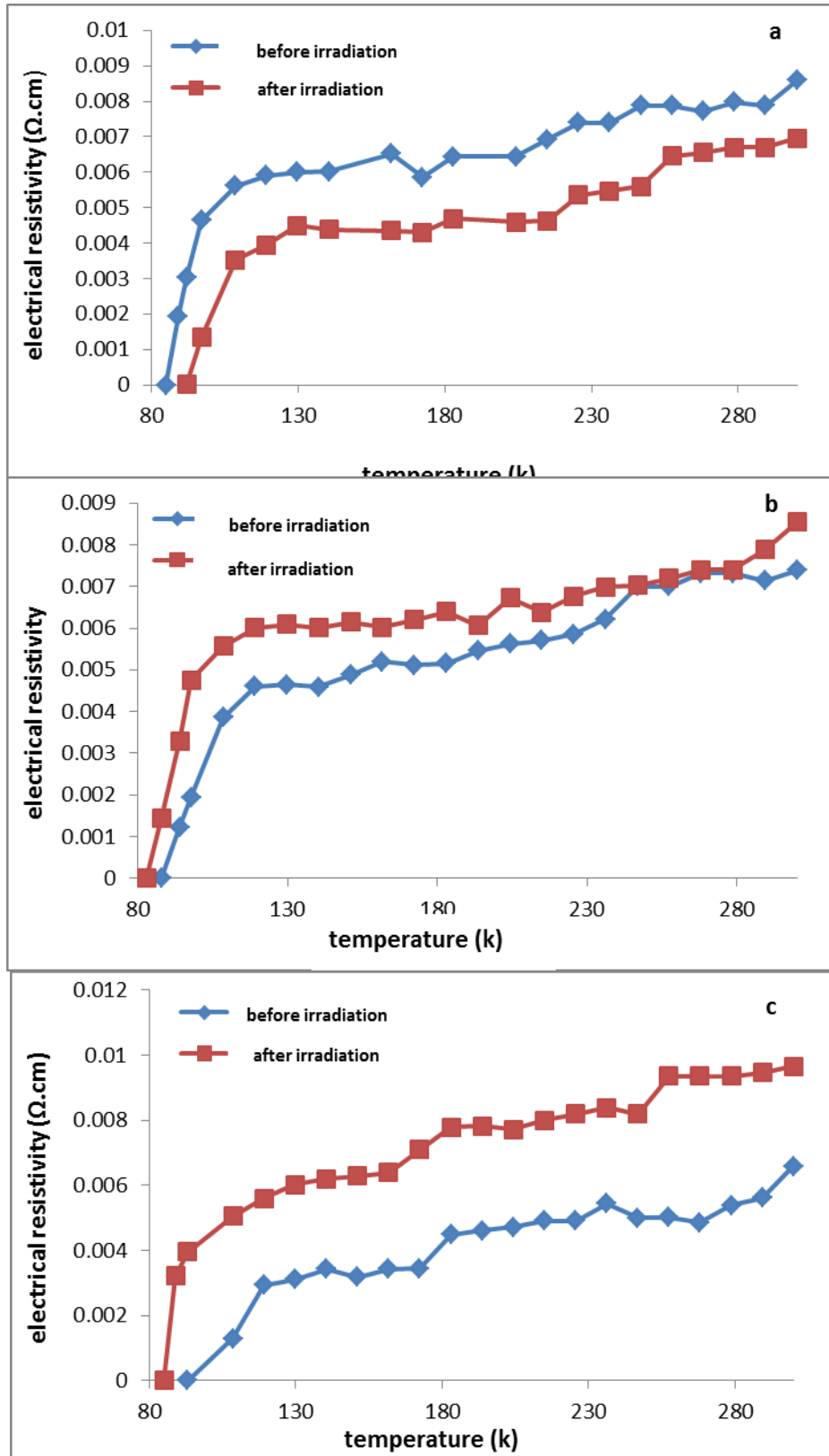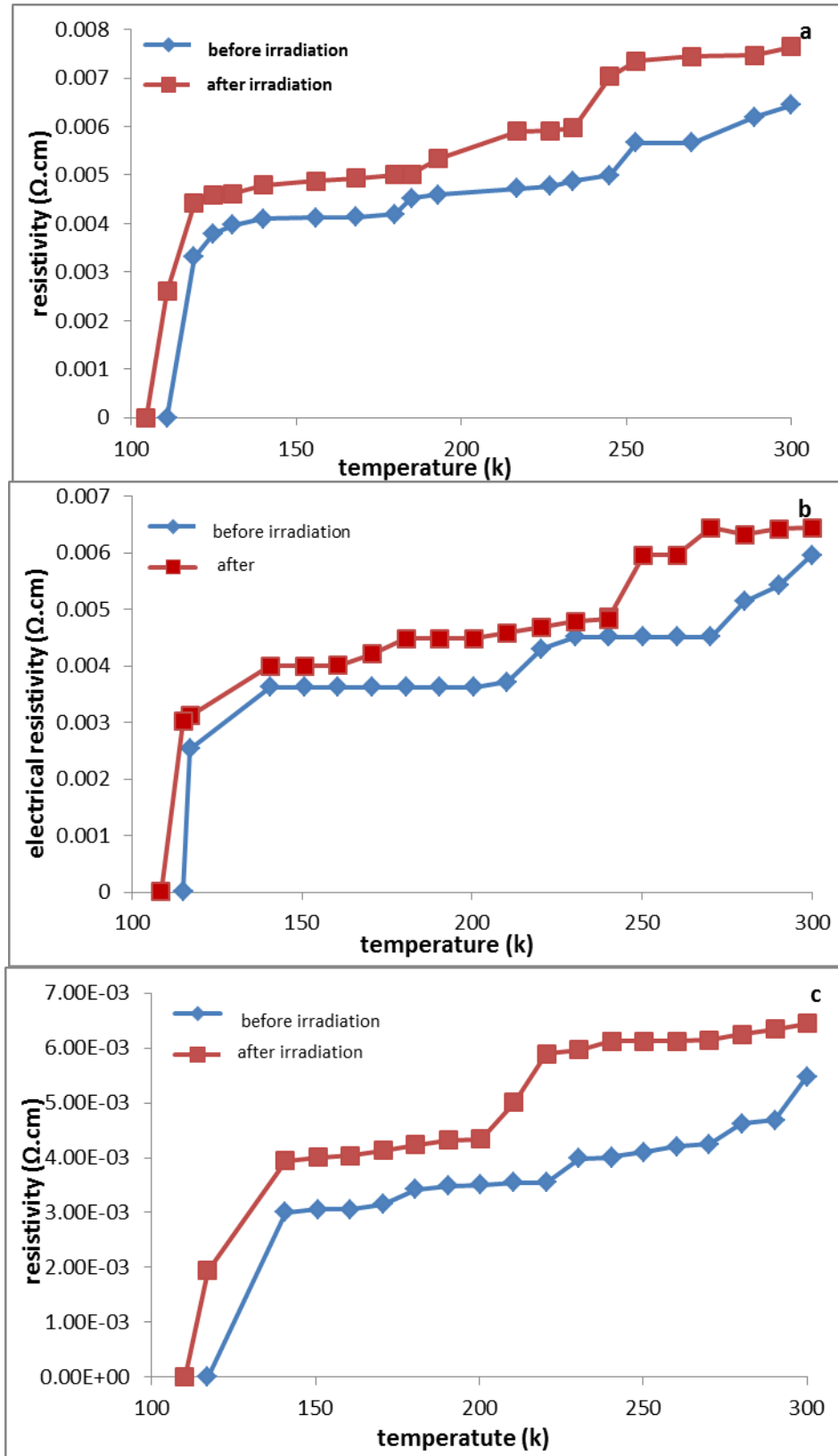
Figure4- 16:Absolute temperature vs. electrical resistivety of
$Bi_{2-x}Pb_xSr_2Ca_2\ Cu_{3-y}Ni_yO_{8+\delta}$**specimens after exposed to fast neutron**
irradiation with substitution concentration (a:x=y=0)(b:x=y=0.2) and (x=y=0.4).

4.4.3Laser ray effect on critical temperature of fabricated specimens:

Four probes test results explained that $Bi_{2-x}Pb_xSr_2Ca_{n-1}Cu_{n-y}Ni_yO_{2n+4+\delta}$ (n=2and3) specimens with substitution concentrations (x=y=0, 0.2 and 0.4) exhibited changes due expose to laser ray, where it is noted that $Bi_2Sr_2Ca\,Cu_2O_{8+\delta}$ $Bi_{1.8}Pb_{0.2}Sr_2Ca\,Cu_{1.8}Ni_{0.2}O_{8+\delta}$, $Bi_2Sr_2Ca_2\,Cu_3O_{10+\delta}$ and $Bi_{1.6}Pb_{0.4}Sr_2Ca_2\,Cu_{2.6}Ni_{0.4}O_{10+\delta}$ specimens exhibits increase in its critical temperature by approximately 7K, 5K, 11K and 2K respectively after expose irradiation as illustrated in Figures (4-17) and (4-18). These increases may be happened because that the crystalline structure of the specimen's compound continues in the state of uniformity produce increase in C-axis length which enhances T_C [59]. This means that laser irradiation serves as thermal treatment source, so the oxygen content increased as explained in iodometric test, and enhanced crystal structure as illustrated in x-ray diffraction test, where volume fraction V_{ph} of high T_c phase (2212) in (n=2) specimens and 2223 in (n=3) specimens), so critical temperature increased as explained in a result.

For $Bi_{1.6}Pb_{0.4}Sr_2Ca\,Cu_{1.6}Ni_{0.6}O_{8+\delta}$ and $Bi_{1.8}Pb_{0.2}Sr_2Ca_2\,Cu_{2.8}Ni_{0.2}O_{10+\delta}$ specimens show decreases in theirs T_c by approximately 10k and 16k after exposed to laser irradiation as illustrated in Figures (4-17) and (4-18). These decreases may attributed to crystal structure of high T_c phase uniformity was missed and low T_c phases (2201) in (n=2) specimens and 2212 in (n=3) specimens) as demonstrated in x-ray diffraction results due to decrease in oxygen content as explained in Iodometric test result which play important role in T_c decrease.

Table4- 9:Magnitudes of critical temperatures of all specimens after exposed to laser ray.

Specimen	$T_{c(offset)}$	$T_{c(onset)}$	$T_{c(mid)}$
$Bi_2Sr_2Ca\ Cu_2O_{8+\delta}$	93	98	95
$Bi_{1.8}Pb_{0.2}Sr_2Ca\ Cu_{1.8}Ni_{0.2}O_{8+\delta}$	95	108	101
$Bi_{1.6}Pb_{0.4}Sr_2Ca\ Cu_{1.6}Ni_{0.4}O_{8+\delta}$	87	94	90
$Bi_2Sr_2Ca_2\ Cu_3O_{10+\delta}$	122	130	126
$Bi_{1.8}Pb_{0.2}Sr_2Ca_2\ Cu_{2.8}Ni_{0.2}O_{10+\delta}$	99	117	108
$Bi_{1.6}Pb_{0.4}Sr_2Ca_2\ Cu_{2.6}Ni_{0.4}O_{10+\delta}$	119	140	129

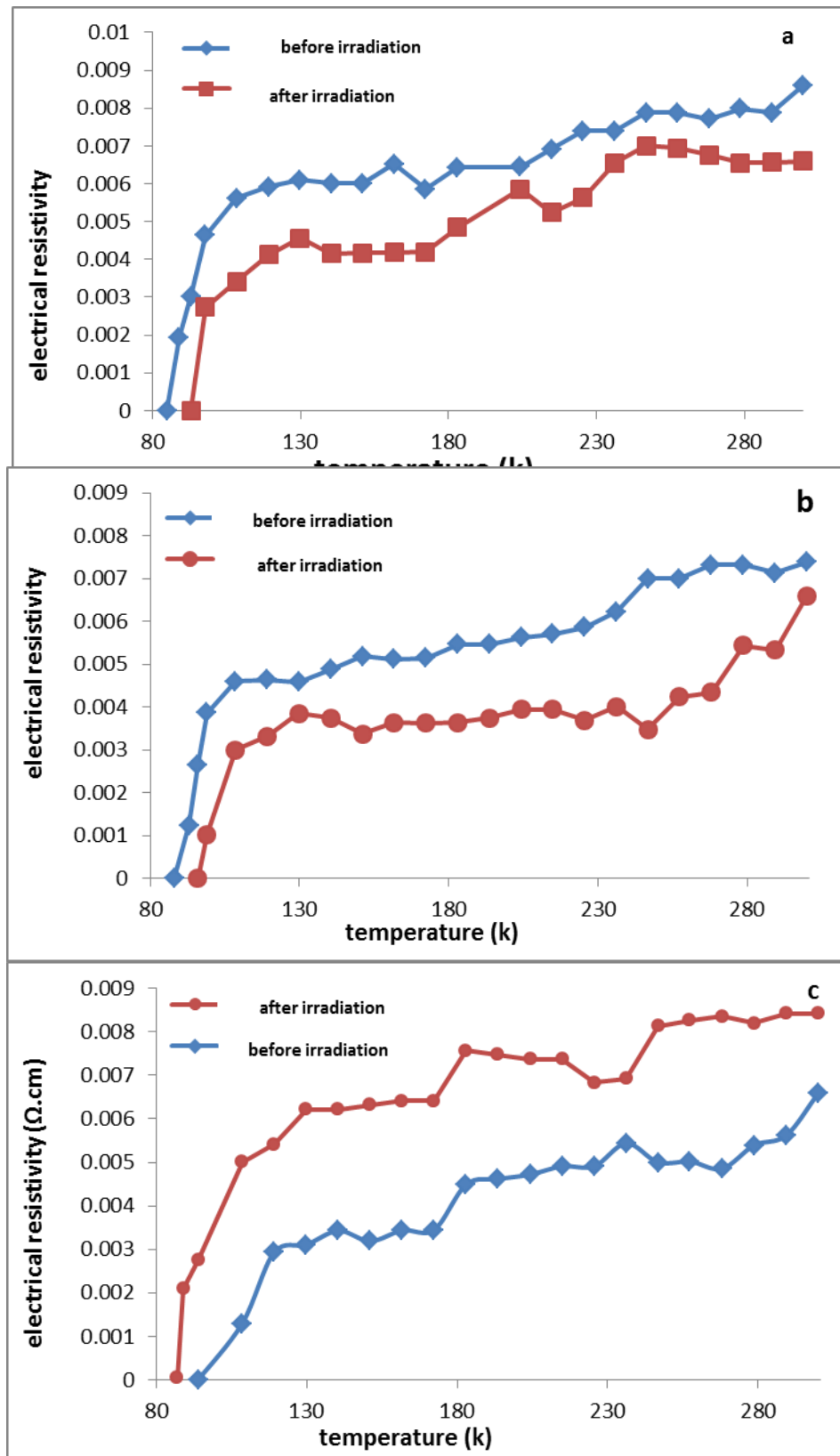**Figure4- 17:Absolute temperature vs. electrical resistivity of**
$Bi_{2-x}Pb_xSr_2Ca_1Cu_{2-y}Ni_YO_{8+\delta}$**specimens after exposed to laser**
irradiation (a:x=y=0)(b:x=y=0.2)(c: x=y=0.4).

Figure4- 18:Absolute temperature vs. electrical resistivity of
$Bi_{2-x}Pb_xSr_2Ca_2Cu_{3-y}Ni_YO_{10+\delta}$**specimens after exposed to laser irradiation**
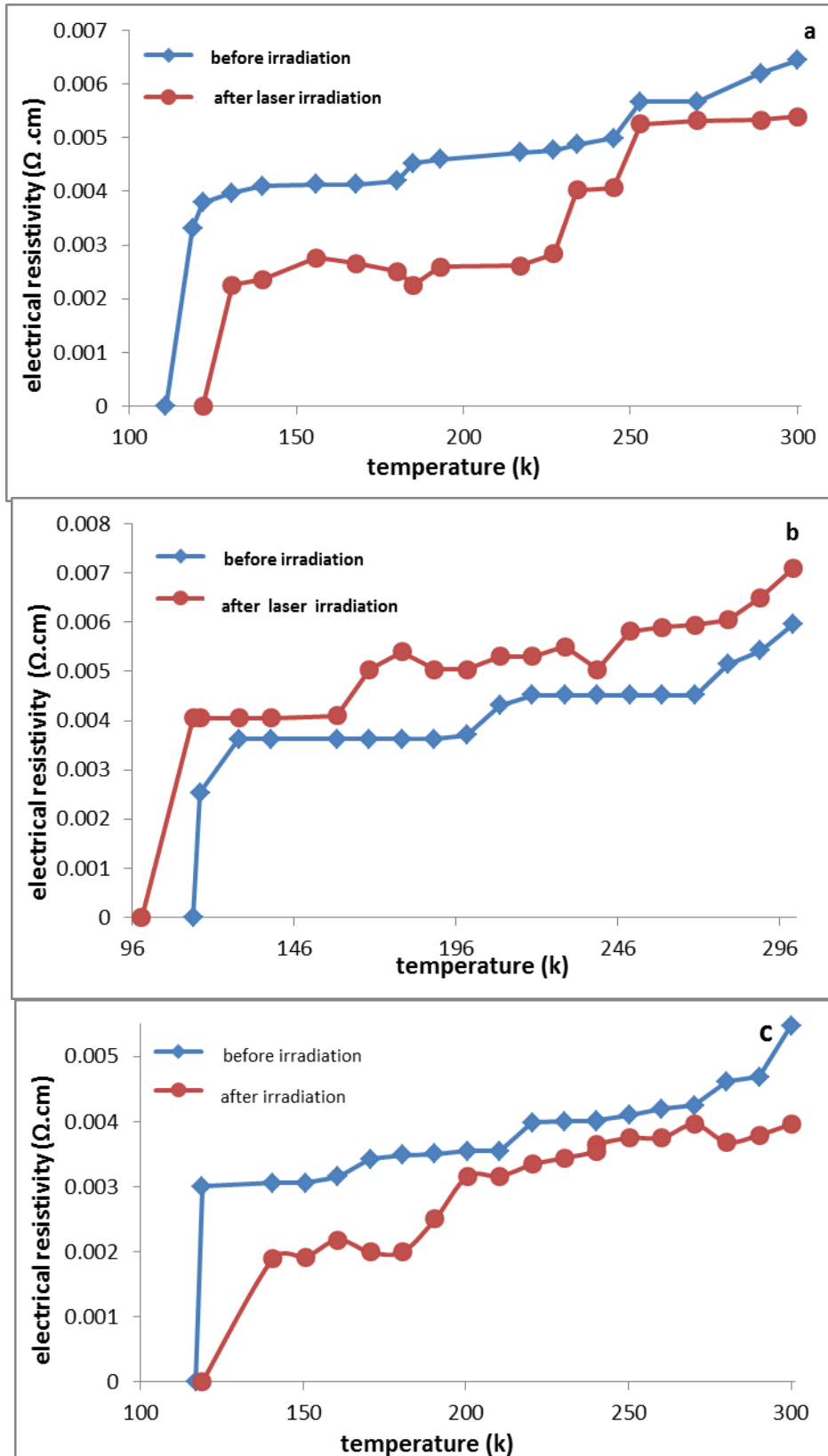**(a:x=y=0)(b:x=y=0.2)(c:(x=y=0.4).**

72

4.4.4 Influence of Beta irradiation on critical temperature of fabricated specimens:

Four probes test results explained that $Bi_{2-x}Pb_xSr_2Ca_{n-1}Cu_{n-y}Ni_yO_{2n+4+\delta}$ (n=2and3) specimens with substitution concentrations (x=y=0, 0.2 and 0.4) exhibited changes due expose to beta irradiation, where it was noted that $Bi_2Sr_2Ca\,Cu_2O_{8+\delta}$, $Bi_{1.8}Pb_{0.2}Sr_2Ca\,Cu_{1.8}Ni_{0.2}O_{8+\delta}$, $Bi_2Sr_2Ca_2\,Cu_3O_{10+\delta}$, $Bi_{1.8}Pb_{0.2}Sr_2Ca_2\,Cu_{2.8}Ni_{0.2}O_{10+\delta}$ and $Bi_{1.6}Pb_{0.4}Sr_2Ca_2\,Cu_{2.6}Ni_{0.4}O_{10+\delta}$ specimens exhibits increase in theirs critical temperatures by approximately 5K, 5K, 6.5K,2K and 7K respectively after expose to beta particles as illustrated in Figures (4-19)and(4-20). These increases attributed to improvement of oxygen content as explained in Iodometric test results, thus high T_c volume fraction phase (2212-phase in (n=2) specimens and 2223-phase in (n=3) specimens) was enhanced as illustrated in x-ray diffraction analysis.

For $Bi_{1.6}Pb_{0.4}Sr_2Ca\,Cu_{1.6}Ni_{0.6}O_{8+\delta}$ specimen show decrease in its T_c by approximately 10k after exposed to beta particles as illustrated in Figure (4-19). These decreases attributed to decrease in oxygen content which was observed in Iodometric test results, thus the low T_c-phase volume fraction (2201-phase in (n=2) specimens and 2212-phase in (n=3) specimens) was decreased.

Table4- 10:Magnitudes of critical temperature of all specimens after exposed to beta irradiation.

specimen	$T_{c(offset)}$	$T_{c(onset)}$	$T_{c(mid)}$
$Bi_2Sr_2Ca\,Cu_2O_{8+\delta}$	98	109	103.5
$Bi_{1.8}Pb_{0.2}Sr_2Ca\,Cu_{1.8}Ni_{0.2}O_{8+\delta}$	96	119	107.5
$Bi_{1.6}Pb_{0.4}Sr_2Ca\,Cu_{1.6}Ni_{0.4}O_{8+\delta}$	84	98	91
$Bi_2Sr_2Ca_2\,Cu_3O_{10+\delta}$	117.5	122	120
$Bi_{1.8}Pb_{0.2}Sr_2Ca_2\,Cu_{2.8}Ni_{0.2}O_{10+\delta}$	126	135	130.5
$Bi_{1.6}Pb_{0.4}Sr_2Ca_2\,Cu_{2.6}Ni_{0.4}O_{10+\delta}$	124	140	132
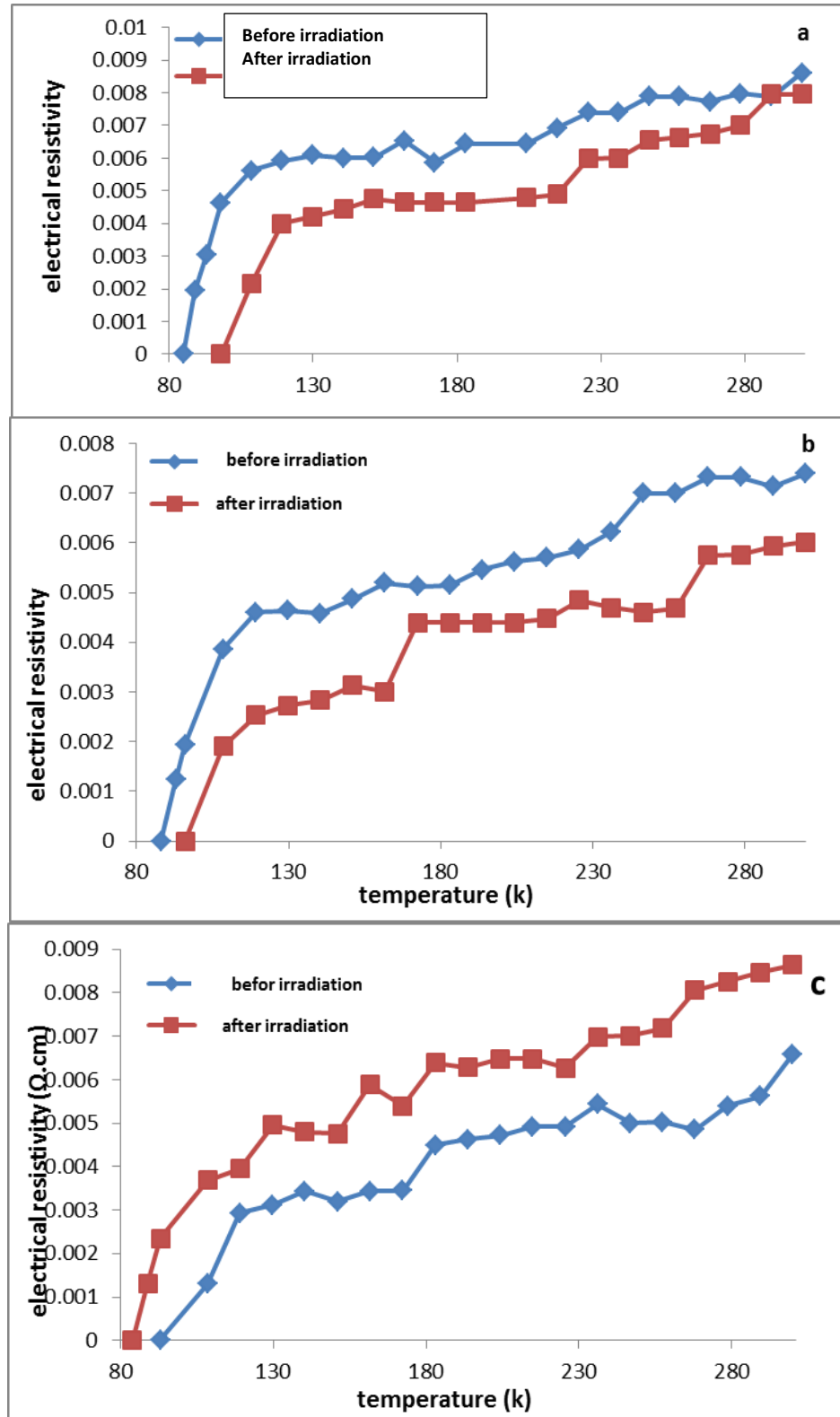
Figure4- 19:Absolute temperature vs. electrical resistivity of
$Bi_{2-x}Pb_xSr_2Ca_1Cu_{2-y}Ni_YO_{8+\delta}$**specimens after exposed to beta irradiation with substitution concentration (a:x=y=0)(b:x=y=0.2)(c:x=y=0.4).**

Figure4- 20:Absolute temperature vs. electrical resistivity of temperature (k)
$Bi_{2-x}Pb_xSr_2Ca_2Cu_{3-y}Ni_YO_{10+\delta}$**specimens after exposed to beta irradiation owith substitution concentration (a:x=y=0)((b:x=y=0.2)and(c:x=y=0.4).**
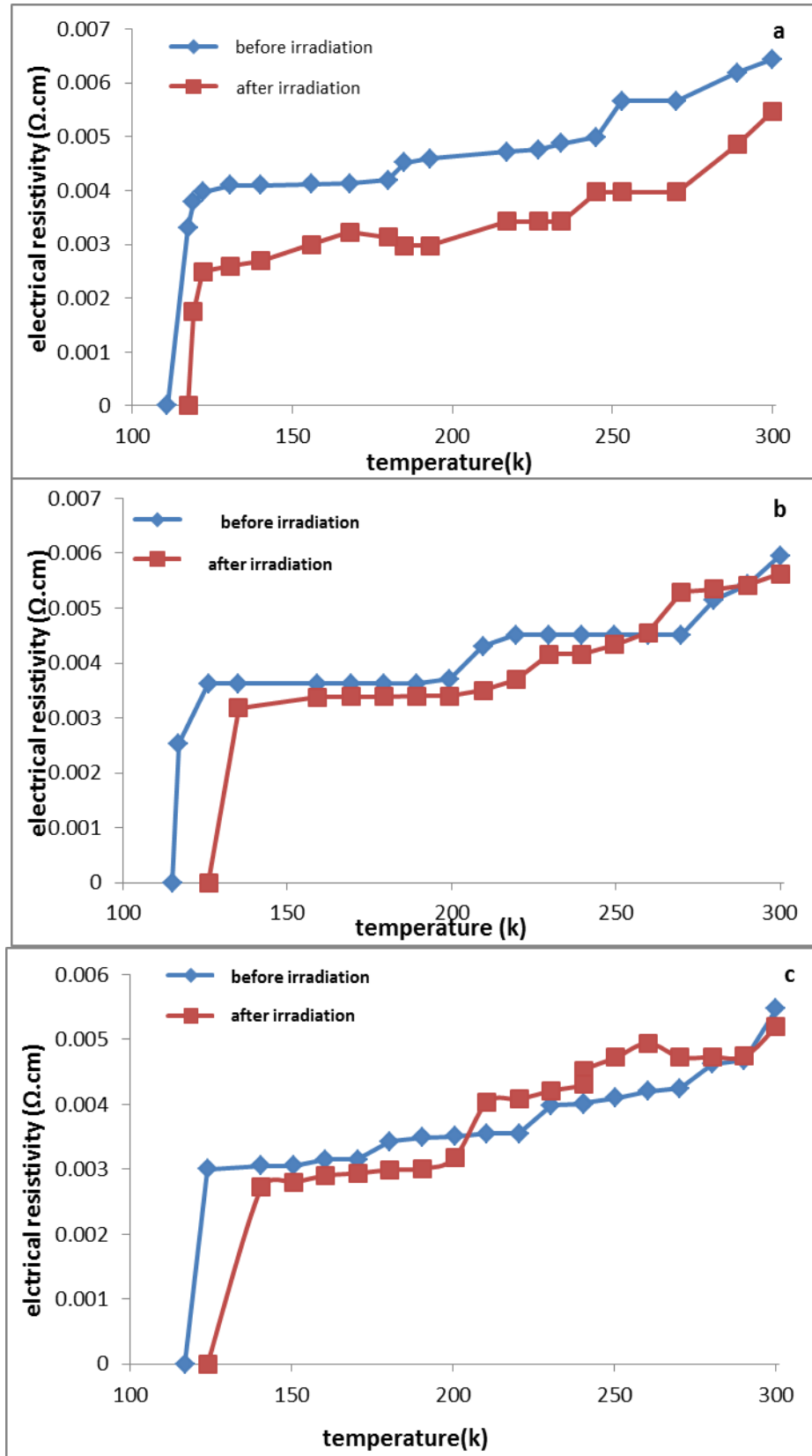
The magnitudes of critical temperature $T_{c(offset)}$ of all fabricated specimens before irradiation, after fast neutron irradiation, after laser irradiation and after beta irradiation were listed in table (4-11) to make the comparison between the influence of all utilized categories of irradiation on fabricated specimens easier and more clear .

Table4- 11:Magnitudes of critical temperature $T_{c(offset)}$ of all specimens before irradiation, after fast neutron irradian, after laser irradiation and after beta irradiation.

specimen	$T_{C(offset)}$ before irradiation	$T_{C(offset)}$ after fast neutron irradiation	$T_{C(offset)}$ after laser irradiation	$T_{C(offset)}$ after beta irradiation
$Bi_2Sr_2Ca\ Cu_2O_{8+\delta}$	85	92	93	98
$Bi_{1.8}Pb_{0.2}Sr_2Ca\ Cu_{1.8}Ni_{0.2}O_{8+\delta}$	88	83	95	96
$Bi_{1.6}Pb_{0.4}Sr_2Ca\ Cu_{1.6}Ni_{0.4}O_{8+\delta}$	93	85	87	84
$Bi_2Sr_2Ca_2\ Cu_3O_{10+\delta}$	111	104.5	122	117.5
$Bi_{1.8}Pb_{0.2}Sr_2Ca_2\ Cu_{2.8}Ni_{0.2}O_{10+}$	115	108.5	99	126
$Bi_{1.6}Pb_{0.4}Sr_2Ca_2\ Cu_{2.6}Ni_{0.4}O_{10+}$	117	110	119	124

.

Chapter five

Conclusions and future works

Chapter Five

Conclusions and future works

5.1 Conclusions:

After reviewing the results of the various tests and their interpretation and discussion it is possible to deduce the following facts:

1- Pb and Ni substitution have very important role in improve the superconductivity of $Bi_{2-x}Pb_xSr_2Ca_{n-1}Cu_{n-y}Ni_yO_{2n+4+\sigma}$ system.

2- The best substitution concentration is (x=y=0.4) for both (n=2) and (n=3) phase, where the critical temperature achieve to 93K and 117K at this concentration for (n=2) and (n=3) respectively.

3- The optimum oxygen content value is (0.4237) for $Bi_{1.6}Pb_{0.4}Sr_2Ca_2Cu_{2.6}Ni_{0.4}O_{2n+4+\sigma}$.

4- X-ray diffraction patterns explained that all fabricated specimens have orthorhombic crystal structure and there are changes in magnitude of lattice parameters due to replacement of Bi and Cu by Pb and Ni.

5- Fast neutron irradiation has a negative influence on superconducting properties of $Bi_{2-x}Pb_xSr_2Ca_{n-1}Cu_{n-y}Ni_yO_{2n+4+\sigma}$ with both two n values and all substitution concentrations expect $Bi_2Sr_2Ca\,Cu_2O_{8+\sigma}$ specimen exhibited enhance its superconductivity, where it exhibited increase in its T_c value, while all other five specimens exhibited decreases in theirs critical temperature .

6- Laser irradiation improve superconducting properties of some specimens and inhibit that of other specimens, where $Bi_{2-x}Pb_xSr_2Ca_{n-1}Cu_{n-y}Ni_yO_{2n+4+\sigma}$ with both two n values and all substitution concentrations improved, expect $Bi_{1.6}Pb_{0.4}Sr_2Ca\,Cu_{1.6}Ni_{0.4}O_{8+\sigma}$ and $Bi_{1.8}Pb_{0.2}Sr_2Ca_2Cu_{2.8}Ni_{0.2}O_{10+\sigma}$, where they exhibited decrease in theirs T_c values, while all other four specimens exhibited increases in theirs critical temperature.

7- Beta irradiation enhances superconducting properties of $Bi_{2-x}Pb_xSr_2Ca_{n-1}Cu_{n-y}Ni_yO_{2n+4+\sigma}$ with both two n values and all substitution concentrations expect $Bi_{1.6}Pb_{0.4}Sr_2Ca\,Cu_{1.6}Ni_{0.4}O_{8+\sigma}$, where it exhibited decrease in its T_c values, while all other five specimens exhibited increases in theirs critical temperature.

<u>Future works:</u>

1- Study influence of gamma irradiation on properties of $Bi_{2-x}Pb_xSr_2Ca_{n-1}Cu_{n-y}Ni_yO_{2n+4+\sigma}$ superconductor system.

2- Study influence of thermal neutron irradiation on properties of $Bi_{2-x}Pb_xSr_2Ca_{n-1}Cu_{n-y}Ni_yO_{2n+4+\sigma}$ superconductor system.

3- Study the influence of fast neutron, laser and beta irradiation on critical current density of $Bi_{2-x}Pb_xSr_2Ca_{n-1}Cu_{n-y}Ni_yO_{2n+4+\sigma}$ superconductor system.

4- Study the influence of fast neutron, laser and beta irradiation on critical dielectric properties of $Bi_{2-x}Pb_xSr_2Ca_{n-1}Cu_{n-y}Ni_yO_{2n+4+\sigma}$ system at room temperature.

5- Study the influence of fast neutron, laser and beta irradiation on mechanical properties of $Bi_{2-x}Pb_xSr_2Ca_{n-1}Cu_{n-y}Ni_yO_{2n+4+\sigma}$ superconductor system.　　　　.

References

<u>References:</u>

[1]   A. S. S. Baki, "Effect of Partial Substitution of Pb on Structural And Electrical Properties of High Temperature Tl2Ba2Ca2Cu3O10+δ," Ph.D. thesis ,The Council College of Education, University of Tikrit ,, 2008.

[2]   N. Q. Raoof, "The Impact of Preparation Condition and Li Substitution on Bi2-x LixPb0.3 Sr2Ca2Cu3O10+ δ compound.," Ph.D. thesis , university of baghdad m college of scince, 2014.

[3]   J.H., Field and H. and Miller "High Temperature Super Conductor materials," Marcel Dekker, Inc, p. 37, 1988.

[4]   H. Onnes, Disappearance of the electrical resistance of mercury at helium temperatures. In Proceedings Koninklijke Akademie van Wetenschappen te Amsterdam, 1911, pp. (pp. 113-115).

[5]   A. M. Ibraheim, "Effect Of Preparation MethodS On The Structural , Mechanical and Electrical Properties Of Effect Of Preparation MethodS On The Structural , Mechanical and Electrical Properties of Bi2Sr2Ca2-xCdxCu3O10+δ System," M.S.C. thesis , university of baghdad , college of education (IBN AL-HAITHAM), 2015.

[6]   J. Horacio. A. Farach. ,. R. Creswick,. R. Prozorov. Charles P. Poole, in superconductivity , second edition , 2007, p. 24.

[7]   J. William and D. Callister ", Fundamentals of Materials Science and Engineering An Interactive",5th edition, John Wiley & Sons, Inc., 2001, p. 289.

[8]   A. Al tland and B. Simons ", A, in concepts of Theoretical solid state physics, 2001, p. 254.

[9]   L.N.Cooper , a. J.R.Schriffer. J. R. ,. J.Bardeen, "Theory of Superconductivity," Phys. Rev, vol. 108, p. 1175, 1957.

[10] B. A. W. AL-JURANI, "charectarization and properties of Hg1-x-yTlxPbyBa2Ca2Cu3O8+δ system," Ph.D. thesis , university of baghdad , college of scince b, 2007.

[11] K.A.Muller:z.,and J.G.Bednorz , Phys.B, vol. 64, p. 189, 1986.

[12] . MK Wu, JR Ashburn, CJ Torng, PH Hor, RL Meng, L. Gao, ZJ Huang, YQ Wang, and CW Chu, Phys. Rev. Lett, vol. 58, p. 908, 1987.

[13] J. Clarke, "Scientific American," SQUIDs, vol. 271(2), p. 46, 1994.

[14] C. Gao ,L. Chen , F. Huang, Z. Meng. R. and.X. Y. Chu, "Superconductivity above 150 K in HgBa2Ca2Cu3O8+δ at high pressures," nature, 1993.

[15] h. sahi, "Preparation and study the effective of addition In and La) on Bi2-x Inx Sr2 Ca2 Cu3-y Lay O10+δ) superconductor compound," Ph.D. thesis university of baghdad , college of education (ibn al-haitham), 2018.

[16] R.S. Liu, J.M. Liang, S.F. Wu, Y.T.Huang and P.T.Wu, Physica C , vol. 159, pp. 385-390, (1981).

[17] C. Kittel, in " Introduction to solid state physics", Seventh edition, 2004, p.17.

[18] Yuan, Y.Jiag and G. X. Yuan, in Applied Physics Letters, 22 MARCH 2004, pp. 2127-2129.

[19] M. G. Yusef, solid state physics, baghdad, 1989.

[20] A. Alexander Al tland and Ben Simons .concepts of Theoretical solid state physics, 2001, pp. 254.

[21] R. W, in " High Temperature Superconductor " , materials properties and Application , New York , Kluwer Academic publishers, 1998 ..

[22] S.O, Pilla, in solid state physics Revised and Enlarged Edition , New

Age International limited , 1995.

[23] C. Gao ,L. Chen , F. Huang, Z. Meng. R. and.X. Y. Chu " Superconductivity above 130 K in the Hg-Ba-Ca-Cu-O system," Nature, vol. vol. 363, pp. 56-58, 1993.

[24] L.N.Cooper , a. J.R.Schriffer. J. R.. Bardeen, "Theory of Superconductivity," Phys. Rev, Vols. 108 , number 5, p. 1175, 1957.

[25] A.B.Pippard, "Proc. Roy. Soc. , A216, 547, , in Ref.26.," London, 1953.

[26] V. a. S.A.Wolf, "Fundamentals of Superconductivity",, New york: Plenum Presses, 1990.

[27] I. a. E. A.C.Rose, "Introduction to superconductivity, Pergamon Press, 1978.

[28] A. a. M.Maqsood, "proceeding of the international workshop held at Rajshahi university," in edited by AKMA Islam, Bangladesh, 28 Oct-1Nov-1996.

[29] S.Chand, in Modern Physics"15th Revised Multicolour Edition, 2010, p. 587.

[30] R. W. G. Ruslan Prozorov, " Magnetic Penetration Depth in Unconventional Superconductors," in Superconductor Science and technology, 2006, p. 3.

[31] A. A. S. E. Kaseh, " Nanolithography, Phd. University of Stellenbosch," Fabrication of Josephon junction using AFM"., 2010.

[32] M. R. Beasley, "Advances in superconductivity," Kitazawa, Ishiguro , 1988, pp. EDS 3-15.

[33] L.D, Ginzburg and Landau, "On The Theory Of Superconductivity Zh. Eksp. Teor. Fiz," vol. 20, p. 1064, 1950.

[34] A,Vladimir, Z.kresin and Stuart"Fundamentals of Superconductivity

" Wolf plenum, pp. 22-24, 1992.

[35] S. H. Mahdi, "Synthesis and study structural, electrical and mechanical properties of composite superconductor.," Ph.D. thesis ,University of Baghdad \College of Education for Pure Science (Ibn-AL-Haitham), 2015.

[36] Y. A. Hamam, A. El Ali (Al-Dairy), K. D. Alazawi and S. M. Mamand., "Effect of Sintering and Annealing Temperatures on the Critical Temperature and Electrical Resistivity of Bi2Ba2Ca2Cu3O10+δ"," Jordan Journal of Physics, vol. 2, pp. 165-170, 2009.

[37] D, Solymar L and Walsh " Ch . 14," in Electrical properties of Materials, oxford university press , 1998.

[38] W. C.S, "Electronic structure , Lattice Dynamics and magnetic Interations in High temperature Superconductivity," springe W.Lynn ,r, 1990.

[39] e. k. a. al-beyaty, "effect of n variation on Tc of (Hg0.8Tl0.2)Ba2Can-1CunO2n+2+δ compound," MS.C. thesis , university of baghdad , college of scince, 2007.

[40] S. Tanaita, ""High-temperature superconductivity: History and out look"," Tanaita SAP international, vol. 4, pp. 10-13, 2001.

[41] K. Likharev, Dynamics of Josephson junctions and circuits. ., Gordon and Breach science publishers, 1986.

[42] n. q. fadhil, "Study the effect of (Y2O3,Sb2O3,SrO) substatution on the structural and electrical properties of the HgBa2Ca2Cu3O8+δ superconductor compound," MS.C. thesis , university of baghdad , college of education of pure scince (IBN AL-HAITHAM), 2016.

[43] S. A. Sunshine, T. Siegrist, L.F. Schneemeyer, D. W. Murphy, R.J. Cava, PHYS.REV, vol. 38, pp. 893, 1988.

[44] E.W, Carlson, "Concepts in High Temperature Superconductivity," 2002, pp. 26-31.

[45] Hazen, R.M., Prewitt, C.T., Angel, R.J., Ross, N.L., Finger, L.W., Hadidiacos, C.G., Veblen, D.R., Heaney, P.J., Hor, P.H., Meng, R.L. and Sun, Y.Y., 1988. Superconductivity in the high-T c Bi-Ca-Sr-Cu-O system: Phase identification. *Physical review letters*, *60*(12), p.1174.

[46] Y. Yamada and S. Murase, Jap. J. Appl. Phys., vol. 27, pp. No.6, L996, 1988.

[47] Z.Quam, H. Shen, Y. Qin, and Y.Jiang, "Jia-Ju. Du, J. Philol. Maga. Lett.," vol. 60, pp. No. 6, p123, 1989.

[48] T. S. K .Kumar, "Ch 10," in Solid State Physics, 2005, pp. 214-216.

[49] M. A. Omer, "ch.10," in Elementary Solid State Physics Principles and Applications, Fifth Impression eddison-Wesley, 2009.

[50] Farbod., M. Z. Shoushtari , S. E. Mousavi Ghahfarokhi and M.., J. Appl. Sci, vol. 8(14), pp. 2613, 2008.

[51] K. A. jassim, "Comparison Study of TC Between the Superconducting Compounds Bi& Hg," Ph.D. thesis ,University of Baghdad, college of scince, 2005.

[52] M. H.J.Maktoof, Ph.D. Thesis,University Of Baghdad Collage Of Sience, 2005.

[53] M. a. hapeep, "Phase Transition of High Temperature Superconductor Bi2-x Pbx Sr2-y (Ba,Sb)y Ca2 Cu3 O10 System .," university of bahgdad , college of scince ,Ph.D thesis , 2006.

[54] H. A.Thabit G.Y.Hermiz and B. A.Aljurani, "Superconducting Properties of the (Bi0. 8Pb0. 2) 2 (Sr0. 9Ba0. 1) 2 Ca2Cu3-x Nix O10+ δ System. ,, .," J. Baghdad Sci, vol. 8, pp. 607-612, 2011.

[55] Ö. Bilgili, K. Kocabaş and E. B.Cevizci , "A Study on Structure of Nb Doped BSCCO Superconductor Compound by X-Ray Diffraction," 3rd Turkish crystallographic meeting,Izmer, 2012.

[56] S. Halim, S. Chen and M. A. Kechik, "AC Susceptibility of Magnesium Diboride (MgB2) Addition in Bi-Pb-Sr-Ca-Cu-O Ceramics Superconductors," 4th International Conference On Solid State Science And Technology , ICSSST, 2012.

[57] S.M .Shaban, (IJAIEM), vol. 2, no. 3, 2013.

[58] T. J. ALWAN, H. M. Louis. and. K. A. JASIM, "The effect of neutron irradiation on the properties of Tl0.6Pb0.3Cd0.1Ba2Ca2Cu3O9−δ superconductors," Turkish Journal of Physics, vol. 37, pp. 237 – 241, 2013.

[59] N. A.W. A. Mohammed, " studying the effect of laser on structural and electrical properties of Ti2-x HgxBa2-ySryCa2Cu3O10+d High temperature superconductor.," MSC thesis , college of education of pure scince , university of tikreet, 2015.

[60] A. Wahab, in Solid State Physics structure and properties of material, Second Edition ., new delhi, 2010, pp. 555-556.

[61] G. Haertling, "DEVELOPMENT OF HIGH Tc (>ll0K) Bi, TI and Y-BASED MATERIALS AS SUPERCONDUCTING CIRCUIT ELEMENTS," clemone university, pp. 2,3, 1994.

[62] J.M.Tarascon, , LePage, Y. Greene, L.H. Bagley, B.G., Barboux, P., Hwang, D.M.Hull, G.W.McKinnon. and Giroud, M., "Origin of the 110-K superconducting transition in the Bi-Sr-Ca-Cu-O system," in Physical Review B, 1988, pp.2504..

[63] J . B .lace, Torrance , Y . Tdkura and J. Lap, solid state comm, vol. 66, pp. 703-706, 1988.

[64] Z. Hong, M. wang, G. Xiong and X. Fan, Physica C, vol. 288, pp. 82, 1997.

[65] N. Q. Raoof, the impact of preparation conditions and Li substitution on Bi2-x LixPb0.3 Sr2Ca2Cu3O10+ δ compound, University of Baghdad college of scince .MCS thesis, 2014.

[66] S. G. G. Subramanian, "Bi-Sr-Ca-Cu-O Thin Films Grown by Flash Evaporation and Pulsed Laser Deposition," M.Sc thesis, Texas University, 2003.

[67] Takehiko, Yag L Ho, Kuzng Mao and Petter, "Transition. Phys and Chems of perovskite," 3, 2, 97 August 28 (1987)..

[68] R. Cloots, M. Ausloss, M. Pekala, A. J. Hurd G. Vacquier and Pavuna,, "Tayloring the properties of layered oxides" in super. Materials, Nato Science series," in ,Kluwer, Netherland, A cademic publishers, 2000.

[69] O. S. M. Salim, "effect of substitution of cu on Tc of Bi2-xCuxPb0.3Sr2Ca2Cu3O10+δ superconductors," 2009.

[70] S. M. Shakouli, "fabrication of Bi1.6Pb0.4Sr2Ca2Cu3-xZnxO10+s thin film prepared by pulse laser deposition method," in Ph.D.thesis , university of baghdad , college of scince , 2013.

[71] B. Batlog, T.T.M. Palstra , L.F. Schneemeyer, R.B.Van Dover and R.J. Cava, Physica C, vol. 153, p. 1062, 1988.

[72] B. A. W. A. Jorani, "Characterization and Properties of the Superconducting system," ph.D theaisis ,university of baghdad, pp. 120-121, 2007.

[73] D.Allender, J.Bray and J.Bardeen, Phys.Rev., B, vol. 7, p. 1020, 1973.

[74] Z.-S. Wang, "SUPERCONDUCTING PROPERTIES OF IRON-BASED BA-122 BY TRANSPORT MEASUREMENTS AND SCANNING NANO-SQUID MICROSCOPY," Universit´e Joseph-Fourier - Grenoble I, p. 6, 2012.

[75] K.A. Jassim, " Fabrication and characterization of (Hg, Bi)-Doped of Tl based Superconducting System (Doctoral dissertation," Ph. D Thesis, Baghdad University, College of Science, 2007.

[76] S.Okayasu, Y.Kazumata and S.Okayasu, "Radiation Effect in Bismuth-Based High-temperature superconductor," p. 177, 1996.

[77] M. H. M.C.Frischherz, Physica-C, vol. 232, p. 309, 1994.

[78] R.A.Sutton,and M.E.Mchenry , Materials Science, vol. 38, p. 159, 1994.

[79] S.J. Mantan and C.Beduz, Materials Science and Engineering B-Solid state materials for advanced technlogy, vol. 53, p. 182, 1997.

[80] H. S. Hussain, "investigation of particles distribution and matrix types for gamma and beta irradiated lead polymer composites," Ph.D. thesis , university of baghdad college of scince , p. 50, 2011.

[81] Sugioka, K., Meunier, M. and Piqué, A. eds., 2010. Laser precision microfabrication (Vol. 135). Springer.

[82] I. F. Ferguson and A. H. Rogerson, " Comput. Phys.," Commun., vol. 32, p. 95, (1984).

[83] L. Abbas, " Effect of Ag and In Substitution on Tc and superconducting Properties of the Hg1-x (Ag, In) xBa2-ySryCa2Cu3O8+ δ," Doctoral dissertation, Ph. D Thesis, University of Baghdad, 2006.

[84] Y . I keda, M . Takano , Z . Hiroi , K . Oda , H . Kitaguchi , J . Takada , O . Yamamoto and H . Mazaki, Jpn . J . Appl . phys, vol. 27, p. 372, 1988.

[85] K. Park, " " Magnetic Phase Diagram of Ca2+xY2−xCu5O10−δ : Oxygen Hole-Doping Effects," THE UNIVERSITY OF TEXAS AT AUSTIN, pp. 36, 84 , 85, 2007.

[86] P. P . Satreand A . Sebaoun and O . Monnereau and G . Vacquier, ".," J . phys . I I I France, vol. 4, p. 261, 1994.

[87] Q. Y. Hu, H.W. Weber, F. M. Sauerzopf, G. W. Schulz and R. M. Schalk,, Appl. Phys. Lett, pp. 65, (1994), 3008, 1994.

[88] F. M.Sauerzopf, H.P.Wiesinger,W. Kritscha, H.W. Weber, M.C.Frischherz,. and Gerstenberg, , " Fast neutron irradiation and flux pinning in single crystalline high temperature superconductors," Cryogenics, vol. 33(1), pp. pp.8-13., 1993..

[89] B. S.Mitchell, in An Introduction to materials Engineering And Science, , Wiley , inc, 2004, p. 45.

الخلاصة:

تتضمن هذه الرسالة تحضير النظام فائق التوصيل بدرجات الحرارة العالية ذو الصيغة الكيميائية

$Bi_{2-x}Pb_xSr_2Ca_{n-1}Cu_{n-y}Ni_yO_{2n+4+\sigma}$ حيث (n=2, 3) و(x=y=0,0.2,0.4)،

حيث تم تحضير اربع عينات لكل قيمة n ولكل قيمة نسبة استبدال (x,y) وتم دراسة تأثير

اصناف مختلفة من الاشعاع على العينات المحضرة. العينة الاولى لم يتم تعريضها لأي صنف

من الاشعاع و العينة الثانية تم تعريضها أشعاع النيوترونات السريعة بأستخدام مصدر $Am^{241}/$

Be بفيض مقداره $1.296 * 10^{11}$neutron/cm^2 و العينة الثالثة تم تعريضها لاشعاع

الليزرباستخدام مصدر ليزر ثنائي القطب بقدرة (150mw) والرابعة تم تعريضها لاشعاع

جسيمات بيتا باستخدام مصدر Sr^{90}/Y^{90} بجرعة مقدارها Gy $887.08*10^8$.

تبين من اختبار حيود الاشعة السينية ان كل العينات التي تم تحضيرها تملك نظام بلوري معيني

قائم (orthorhombic) متعدد الاطوار، حيث ان العينات (n=2) هنالك طوررئيسي

(2212)وطور ثانوي (2201) وفي العينات (n=3) هنالك طور رئيسي (2223) وطور ثانوي

(2212) ، بالاضافة لنسبة ضئيلة من طور غير معروف.وأن عملية الاستبدال ادت الى تغييرات

في قيم كل من ثوابت الشبيكة و حجم خلية الوحدةو النسب الحجمية لتشكيل الاطوار والكثافة

الكتلية والحجم البلوري لكل العينات المحضرة.

تم استخدام تقنية المجسات الاربعة لتحديد درجات الحرارة الحرجة للعينات المحضرة وتم

استخدام طريقة المعايرة اليودومترية (التسحيح) لتقدير قيم محتوى الاوكسجين في العينات

المحضرة.

أعلى درجة حرارة حرجة تم الحصول عليها كانت 117K للعينة $Bi_{2-x}Pb_xSr_2Ca_2 Cu_{3-y}Ni_yO_{10+\delta}$

(n=3) و(x=y=0.4) و 93K للعينة $Bi_{2-x}Pb_xSr_2Ca Cu_{2-y}Ni_yO_{8+\delta}$ (n=2) و(x=y=0.4).

قيمة محتوى الاوكسجين الامثل كانت (0.4237) للعينة $Bi_{1.6}Pb_{0.4}Sr_2Ca_2 Cu_{2.6}Ni_{0.4}O_{10+\delta}$ و (0.06092) للعينة $Bi_{2-x}Pb_xSr_2Ca Cu_{2-y}Ni_yO_{8+\delta}$.

تمت دراسة تاثير كل من اشعاع النيترونات السريعة و اشعاع الليزر و اشعاع بيتا على العينات المحضرة ، لم تتم ملاحظة اي تحول طوري ، وتم ملاحظة تغيير في قيم ثوابت الشبيكة و حجم خلية الوحدة و الكثافة الكتلية و الحجم البلوري ودرجة الحرارة الحرجة و قيمة محتوى الاوكسجين ، حيث ان هذه القيم ازدادت في بعض العينات وانخفضت في البعض الاخر بعد التشعيع بصنف من اصناف الاشعاع المذكورة اعلاه . أعلى درجة حرارة حرجة تم الحصول عليها بعد التشعيع بالنيترونات السريعة هي 110K للعينة $Bi_{1.6}Pb_{0.4}Sr_2Ca_2 Cu_{2.6}Ni_{0.4}O_{10+\delta}$. أعلى درجة حرارة حرجة تم الحصول عليها بعد التشعيع هي 122K للعينة $Bi_2Sr_2Ca_2 Cu_3O_{10+\delta}$. أعلى درجة حرارة حرجة تم الحصول عليها بعد التشعيع ببيتا هي 126K للعينة $Bi_{1.8}Pb_{0.2}Sr_2Ca_2 Cu_{2.8}Ni_{0.2}O_{10+\delta}$.

تحضير و دراسة تأثير الاشعاع على الموصل الفائق عند درجات الحرارة العالية
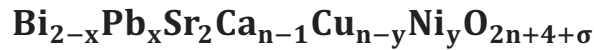
$$Bi_{2-x}Pb_xSr_2Ca_{n-1}Cu_{n-y}Ni_yO_{2n+4+\sigma}$$

رسالة مقدمـة الى

مجلس كليــة التربيــة للعلوم الصرفة / أبــن الهيثم – جـامعـة بغـداد

وهي جـزء مــن متطلبات نيل درجــة الماجستيــر في

علــوم الفيزيـــاء

تقدم بها الطالب

محمد عبد المحسن علي

بإشراف

أ. د. كريم علي جاسم